Applications of artificial intelligence in water treatment for optimization and automation of adsorption processes

Journal Pre-proofs

Review

Applications of artificial intelligence in water treatment for the optimization and automation of the adsorption process: Recent advancesandprospects

Gulzar Alam, Ihsanullah Ihsanullah, Mu. Naushad, Mika Sillanpä ä

PII: S1385-8947(21)01596-5
DOI: https://doi.org/10.1016/j.cej.2021.130011
Reference: CEJ 130011

To appear in: *Chemical Engineering Journal*

Received Date: 19 December 2020
Revised Date: 20 March 2021
Accepted Date: 19 April 2021

Please cite this article as: G. Alam, I. Ihsanullah, Mu. Naushad, M. Sillanpä ä, Applications of artificial intelligence in water treatment for the optimization and automation of the adsorption process: Recent advancesandprospects, *Chemical Engineering Journal* (2021), doi: https://doi.org/10.1016/j.cej.2021.130011

Applications of artificial intelligence in water treatment for the optimization and automation of the adsorption process: Recent advances and prospects

Gulzar Alam[a], Ihsanullah Ihsanullah[b*], Mu. Naushad[c,d,e*], Mika Sillanpää[f,g]

[a] School of Computing, Ulster University, Newtownabbey, Northern Ireland, United Kingdom

[b] Center for Environment and Water, Research Institute, King Fahd University of Petroleum and Minerals, Dhahran 31261, Saudi Arabia

[c] Department of Chemistry, College of Science, King Saud University, Riyadh-11451, Saudi Arabia

[d] Yonsei Frontier Lab, Yonsei University, Seoul, Korea

[e] International Research Centre of Nanotechnology for Himalayan Sustainability (IRCNHS), Shoolini University, Solan, Himachal Pradesh, 173229, India

[f] School of Civil Engineering and Surveying, Faculty of Health, Engineering and Sciences, University of Southern Queensland, West Street, Toowoomba, 4350 QLD, Australia

[g] Department of Chemical Engineering, School of Mining, Metallurgy and Chemical Engineering, University of Johannesburg, P. O. Box 17011, Doornfontein 2028, South Africa

Corresponding Authors' email: engr.ihsan.dir@gmail.com; ihsankhan@kfupm.edu.sa (Ihsanullah Ihsanullah); mnaushad@ksu.edu.sa (M. Naushad)

Abstract

Artificial intelligence (AI) has emerged as a powerful tool to resolve real-world problems and has gained tremendous attention due to its applications in various fields. In recent years, AI techniques have also been employed in water treatment and desalination to optimize the process and to offer practical solutions to water pollution and water scarcity. Applications of AI is also expected to reduce the operational expenditures of the water treatment process by decreasing the cost and optimizing chemicals usage. This review summarizes various AI techniques and their applications in water treatment with a focus on the adsorption of pollutants. Numerous AI models have successfully predicted the performance of different adsorbents for the removal of numerous pollutants from water. This review also highlighted some challenges and research gap concerning applications of AI in water treatment. Despite several advantages offered by AI, there some limitations that hindered the widespread applications of these techniques in real water treatment. The availability and selection of data, poor reproducibility, less evidence of applications in real water treatment are some key challenges that need to be addressed. Recommendations are made to ensure the successful applications of AI in future water-related technologies. This review is beneficial for environmental researchers, engineers, students, and all stakeholders in the water industry.

Keywords: Artificial intelligence; Water treatment; Adsorption; Machine learning; Water pollution; Clean water

1. Introduction

Access to clean drinking water is the grand challenge of the modern era and a prime component of the UN sustainable development goals (SDGs) [1]. On the other hand, water pollution caused by rapid industrialization and population growth has emerged as a grand environmental challenge in recent years [2,3]. Treatment and reuse of wastewater offer a unique opportunity to address both these challenges. Tremendous progress has been made in the past few decades towards the development of novel efficient, and cost-effective techniques for the removal of various pollutants from wastewater [4–8]. The applications of various optimization and modelling tools have also gained considerable attention in recent times for assessing performance and improving efficiency.

Artificial intelligence (AI) is the core and well-known branch of computer science that deals with building smart systems and resolves problems in a manner comparable to the human intelligence system. The primary motive of AI applications to a system is to enhance computer functions that are relevant to human knowledge, such as learning, problems solving, reasoning and perception [9]. AI is a fast-growing field and having real-world applications in diverse fields such as healthcare, smart cities and transportation, e-commerce, finance, and academia [10]. AI is further classified into machine learning, deep learning and data analytics. These techniques are mainly used for intelligent decision-making, blockchain, cloud computing, the internet of things and the fourth industrial revolution (Industry 4.0) [11]. AI is booming mainly due to its unique features to learn and adapt a system based on historical data and to make a decision. AI's significance is rising incessantly with time due to the integration of AI-based systems with intelligence, adaptability and intentionality in their proposed algorithms [12].

AI systems are applicable to almost all interdisciplinary fields, and they have played their potential role in various applications for optimization, classification, regression, and forecasting. AI tools are sometimes used in combination with experimental design techniques such as response surface methodology (RSM) to further enhance the precision of optimal solution prediction.

The application of AI is emerging in water treatment to overcome the complications of traditional methods. In the current era, water industries are investing in artificial intelligence, and according to market research, this investment is expected to reach $6.3 billion by 2030 [13]. Similarly, AI is expected to save 20 to 30 % of operational expenditures by decreasing the cost and optimizing the usage of the chemical in water treatment [14]. The applications of AI in water treatment have made the process easy due to its modest implementation, flexibility, generalization, and design simplicity. The commonly used AI techniques in water treatment are Recurrent Neural Network (RNN), Convoluted Neural Network (CNN), Decision Tree (DT), Feed Forward Back-Propagation Neural Network (FFBPNN), and Adaptive Network Based Fuzzy Inference System (ANFIS). The applications of several hybrid techniques such as ANN-GA, MLP-ANN, ANN-PSO, PSO-GA, Back Propagation (BP)-ANN, Feed Forward Back Propagation (FFBP-ANN), AND Support Vector Regression (SVR)-GA have also been studied in water treatment. The availability of data is the main challenge in applications, as AI needs sufficient historical data to predict future outcomes and offer improvement in the system.

Various studies demonstrated the successful applications of different AI tools for the modelling and optimization of the water treatment process, such as pollutants removal from water [15,16]. However, still, various hurdles hinder the application of AI in water purification. This review provides a critical analysis of different AI tools used for assessing the performance of the

adsorption process employed for the removal of metals, dyes, organic compounds, nutrients, pharmaceuticals, drugs, pesticides, and personal care products (PCPs) from the water. The input variables that affect the process performance are also described, and the parameters that assess the efficiency of AI models are also discussed. Finally, the significant challenges in the widespread applications of AI in water treatment and recommendations for future research are also provided.

2. AI techniques

The most commonly employed AI-based techniques for water treatment are shown in **Fig. 1.** These techniques are extensively used to manage wastewater treatment operations, water reuse, water-saving and cost reduction through prediction, diagnosis, assessment and simulation [16].

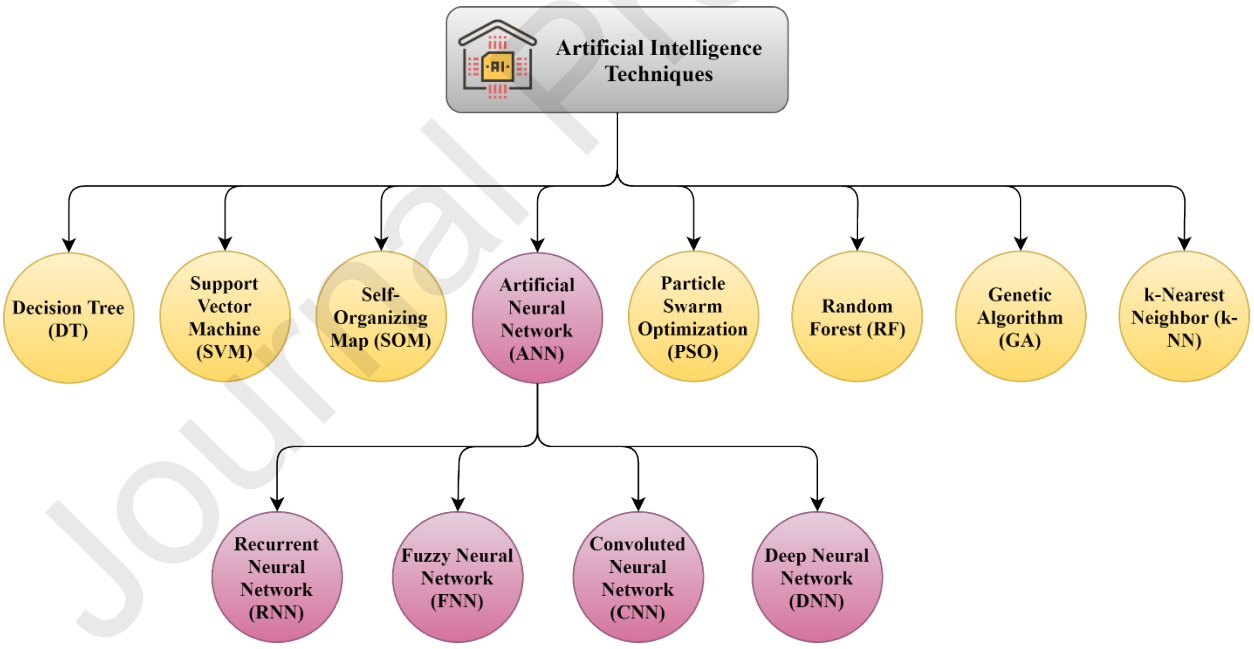

Fig. 1. Classification of AI techniques

2.1. k-Nearest Neighbor (k-NN)

k-NN is a simple machine learning technique used for regression and classification. k-NN save all the existing data and perform classification on new data points on the basis of similarity [17]. For example, consider a classification problem having two categories W and Z, as shown in **Fig. 2.** If a new data point occurred, having a placement issue with W and Z category, the new data point should be placed in a suitable category based on calculating Euclidean distance. Therefore, the new point will be added to category Z that have the maximum number of neighbours. k-NN is the most commonly used technique used for classification problem.

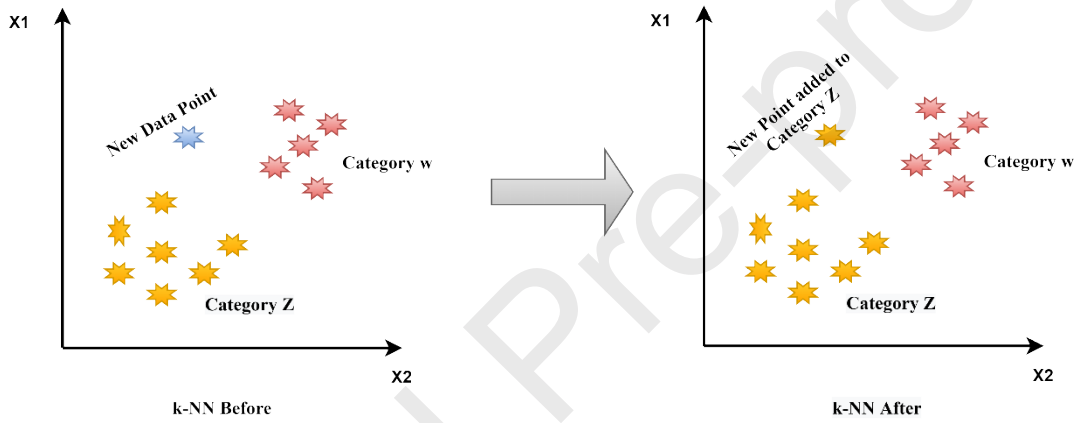

Fig. 2. An example k-NN technique before and after a classification problem

2.2. Decision Tree (DT)

DT technique is mainly used by AI experts for classification and regression problems. The core purpose of DT is to generate a training model used for class prediction by including "learning simple decision rules". It follows a tree structure in which each tree has a node that represents the attribute or feature of the data, the edge represents the probable answers to a problem, and the leaf node denotes the real output or class label [18]. This technique is mostly favoured because of its high accuracy and easy implementation. As depicted in **Fig. 3,** the process may result in

many possible solutions. In a DT technique, all features of a problem are considered from root to leaf node in order to detect the optimal solution based on defined conditions.

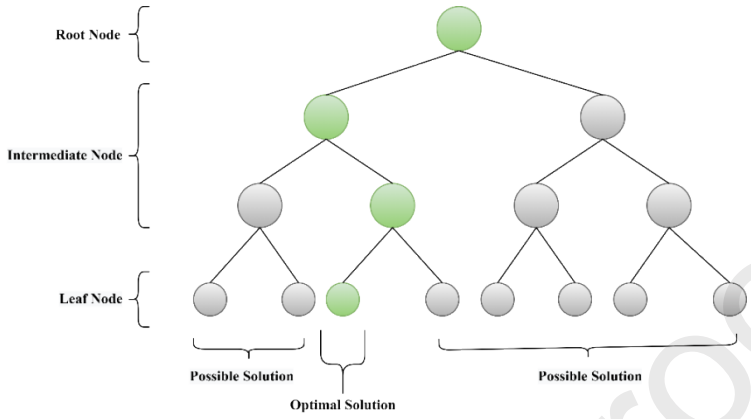

Fig. 3. DT architecture

2.3. Random Forest (RF)

RF is used for both classification and regression problems. Just like the forest, more decision trees means that robust will be the RF. It creates DTs on data samples, and then make a prediction on each DT and lastly, choose the optimal solution based on the voting mechanism [19]. The benefit of using RF is that it decreases the overfitting of the DTs by averaging their result. As shown in **Fig. 4**; the random samples from a given dataset are chosen, and a decision tree is built for each sample. Then, the result of each decision tree is obtained. The next step is to perform the voting process for each predicted result and decide the most voted predicted result as a final result.

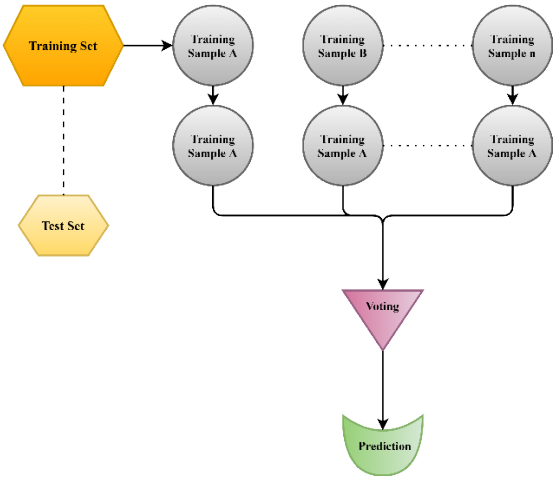

Fig. 4. Typical architecture and working procedure of RF technique

2.4. Artificial Neural Networks (ANNs)

ANNs are the statistical models that are built based on biological human brain neuron to perform parallel and complex computations. It is used mainly for pattern recognition problems to execute modelling and processing nonlinear relationships between the inputs and outputs in a parallel manner. In ANNs, the neuron represents a node, and the activation functions such as sigmoid and hyperbolic are used to perform nonlinear computation [20]. ANNs includes weights between neurons (nodes) that can be changed with respect to a machine learning algorithm by using a suitable cost function to learn from the observed data in order to improve the model. ANNs consists of many layers in which the first layer represents an input layer, the last layer represents the output layer, and the layers present between the first and last layers are the hidden layers. An increase in the number of hidden layers can build complex models that can be trained to improve the performance of ANNs [21]. **Fig. 5** shows a simple architecture of ANNs, including the input layer (a, b, c…n), two hidden layers (hidden layer 1 and 2), and the output layers (a, b…. n). The subtypes of ANNs are discussed below.

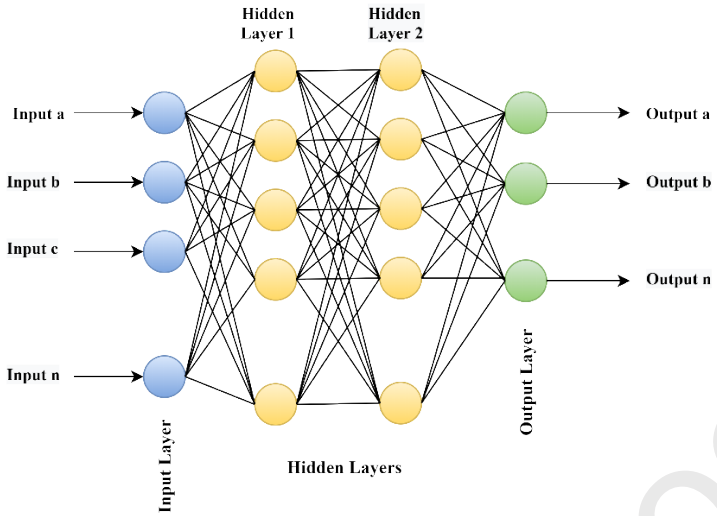

Fig. 5. A basic ANNs with four layers: an input layer, two hidden layers and an output layer

2.4.1. Fuzzy Neural Network (FNN)

FNN is an AI technique developed from the grouping of two fields, fuzzy logic and neural network. FNN detects parameters of a fuzzy system, including fuzzy sets and fuzzy rules, by manipulating the approximation techniques from neural networks. FNN is mainly used for pattern recognition, regression and density estimation in a condition where no mathematical model exists for a specified problem [22].

2.4.2. Convoluted Neural Network (CNN)

CNN is a commonly used class of ANNs that utilize the convolution as an alternative to general matrix multiplication in at least one of their layers and generally known as the feed-forward neural network (FFNN) [23]. CNN is mainly used for image/video recognition and classification, financial time series and natural language processing. Three basic concepts that are used for CNN are "local sparse connections amongst consecutive layers, weight sharing and pooling" [24]. The first two concepts are used for reducing the number of training parameters, and pooling

is using for feature size reduction [25]. The typical architecture of CNN is presented in **Fig. 6**. CNN is composed of two parts: the hidden layers (convolutional and pooling layers), responsible for complex feature extraction, and the classification layers (fully connected and output layers), which is responsible for giving the decision based on parameter learned from the previous layers.

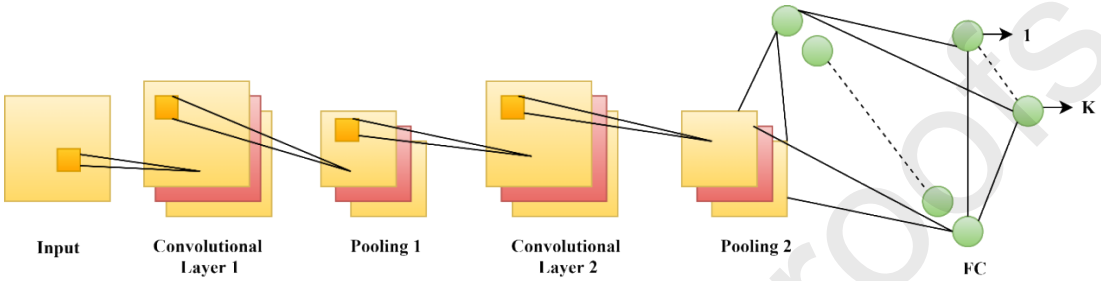

Fig. 6. Basic CNN architecture

2.4.3. Deep Neural Network (DNN)

DNN includes multiple hidden layers along with input and output layers [23,26], as shown in **Fig. 7**. DNN is commonly used for learning complex models and high dimensional data process with the inclusion of more hidden layers and neurons. However, DNN needs additional computing resources and upsurge training difficulties. As compared to other ANNs, DNN provides the best performance if the datasets have enough data [27].

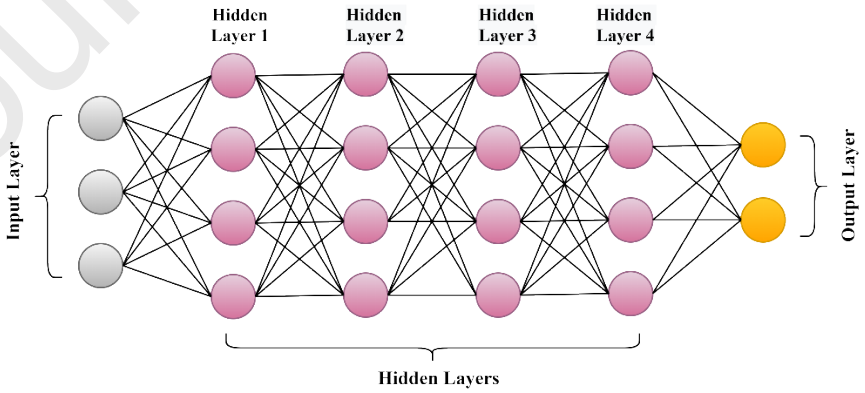

Fig. 7. Common DNN with three input layers, four hidden layers, and two output layers

2.4.4. Recurrent Neural Network (RNN)

RNN is like other ANNs except that it has an additional memory-state to the neurons to share the same parameters. RNN is an FFNN in which the information is transferred from the input layer to the output layer. It saves the output of a specific layer and connecting back to the input for the purpose to predict the output. RNN uses their internal state (memory) to process sequences of inputs with variable-length. The commonly used RNN is long short-term memory (LSTM) that has three gates (the input, output and forger gate) to calculate the hidden state [28]. A simple example of RNN is shown in **Fig. 8,** where nodes in various layers of the neural network are compressed to create RNN of a single layer. The parameters in the proposed RNN are X, Y and Z.

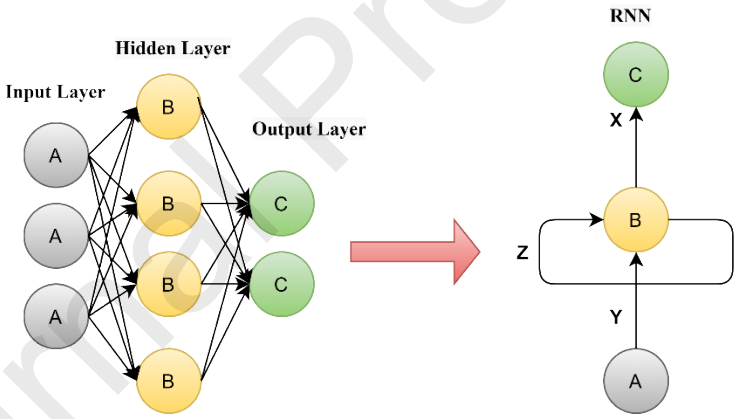

Fig. 8. A typical RNN architecture

2.5. Support Vector Machine (SVM)

SVM is a renowned AI-based technique that is used for solving classification and regression problems. It needs labelled training data for each category to identify the next step. The basic concept of SVM is to map the input vector into a high dimensional feature space. The mapping is

obtained through different kernel functions such as linear, polynomial and radial basis functions, while the function selection is based on datasets [29]. The main purpose of SVM is to differentiate the two classes in the feature space to increase the margin between classes by drawing a hyperplane (as shown in **Fig. 9)**. SVM is mainly used in pattern recognition problems. For example, **Fig. 9** represents the classification of SVM consisting of two classes linear separable via hyperplane. Each class include one support-vector.

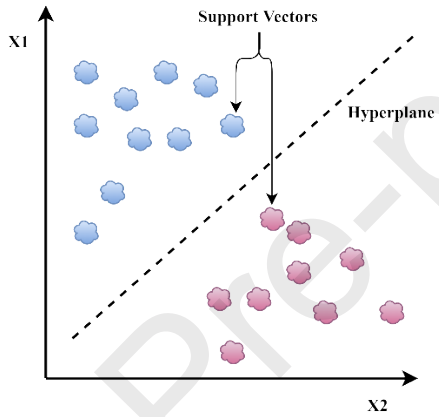

Fig. 9. An example of SVM classification with a linear hyperplane

2.6. Self-Organizing Map (SOM)

SOM is the commonly used AI technique of ANN models. SOM consists of input and output layers. The output layer is also called a feature map or map layer. SOM is mainly used for data clustering and dimensionality reduction, as shown in **Fig. 10**. Weights are directly assigned to the output layer, and every SOM is assigned a weight vector with a similar dimension as the input space. Dimensionality reduction helps to reduce the input variables in a dataset because more features create difficulty in predictive modelling and make it more challenging [30].

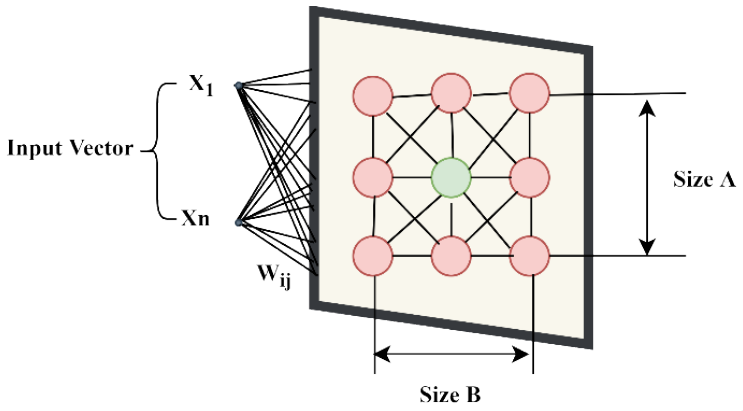

Fig. 10. SOM dimensionality reduction

2.7. Genetic Algorithm (GA)

GA is a heuristic-based search algorithm that acts on a population of possible solutions similar to the biological mechanism of population genetics and selection. It uses a recursive process to achieve the best solution through multiple solutions. In GA, all the possible solutions are encoded as a gene that consists of characters in the form of strings from some alphabets. The new solutions are generated through mutation from the members of the present population, and finally, via mating, two solutions are combined to form a new solution. This algorithm is mainly used to search space for potential solutions and to find the best one by solving a problem [31].

2.8. Particle Swarm Optimization (PSO)

PSO is a commonly used AI-based technique for optimization problems due to its iteration mechanism to improve the solution related to a given quality measure. In PSO, the particles are moving around the search space by considering the velocity and position of the particle. In search space, each particle movement is inclined towards the best-known position, and its position and velocity are updated with time [32]. Every particle is searching for the best position in the search space by changing the velocity according to the defined rule [33]. **Table 1** depicts

the overall defined techniques with their usage domain, advantages, and limitations for each technique.

Table 1. Commonly used AI techniques, their application, advantages and limitations

AI techniques	Applications	Advantages	Limitations
k-NN	Regression, classification	▪ Distance function selection is flexible ▪ Implementation is easy	▪ Distance calculations make it computationally expensive ▪ Memory intensive
DT	Regression, classification	▪ Easy to understand, and data classification is simple ▪ Used for both continuous and discrete data ▪ Capable of choosing the utmost discriminatory feature	▪ Having instability and overfitting
RF	Regression, classification	▪ Good for large scale datasets ▪ Instability is low compared to DT ▪ Lessen the overfitting of DT	▪ Not suitable for imbalanced datasets ▪ Having low training speed
ANN	Regression, classification	▪ Fast prediction ▪ Good for arbitrary function approximation ▪ Good for high dimensional datasets	▪ Computationally expensive, and it is hard to interpret the trained models
SVM	Pattern recognition, regression, classification	▪ Good for high dimensional datasets ▪ Good for linear and nonlinear separable datasets	▪ Hard to train due to large datasets and computationally expensive ▪ Not suitable for noisier datasets because of the overfitting problem
SOM	Clustering	▪ Good for high dimensional datasets ▪ Simple to understand due to its mapping mechanism	▪ Computationally expensive in case of large maps due to more training data

GA	Clustering, regression, classification	▪ Provide more than one solution ▪ Deep domain knowledge is not required ▪ Support multi-objective optimization ▪ Good for discrete and continuous problems	▪ Difficult to implement ▪ Computationally expensive and time-consuming ▪ Fitness function is not defined clearly
PSO	Clustering, regression, classification	▪ Simple to use ▪ Easy to implement ▪ Strong to control parameters ▪ Parallel computation ▪ Computational efficacy compared to other heuristic optimization techniques	▪ Need a mathematical background for evaluation ▪ Difficult to define the initial design parameters
ANN			
FNN	Pattern recognition, regression, classification	▪ No need for a mathematical model ▪ Easy to implement and interpret	▪ Not able to learn ▪ Theoretical knowledge is necessary ▪ Computationally expensive
CNN	Regression, classification, segmentation	▪ Good and accurate results ▪ Good speed because it works in parallel ▪ Capable of extracting important features	▪ Computationally expensive ▪ Complex architecture
DNN	Regression, classification	▪ Good towards nonlinear data ▪ Fast prediction after training ▪ Work well with more data points	▪ Blackbox behavior ▪ Computationally expensive ▪ Require more training data
RNN	Regression, classification	▪ Good for time series prediction ▪ Good for sequence prediction problems ▪ Process inputs of any length can be used	▪ Require more data ▪ Training is difficult ▪ Computationally expensive

2.9. AI hybrid techniques

AI hybrid techniques are a combination of more than one AI technique. Researchers have already employed various hybrid techniques in different fields to get the combined advantages of individual techniques. **Fig. 11** shows four main techniques, GA, PSO, RNN and SVM, that are commonly used in combination with other techniques to attain a more accurate result. Some of the commonly employed hybrid techniques reported in the literature are GA- Multi Layer Perceptron Artificial Neural Network (MLPANN), GA- Radial Basis Function Artificial Neural Network (RBANN), GA- Feedforward Neural Network (FNN) , GA- Fuzzy Logic (FL), SVM-Simulated Annealing (SA), SVM- Adaptive Simulated Annealing Genetic Algorithm (ASAGA), ANN-Differential Evolution (DE), ANN-Genetic Algorithm Neural Network(GANN), PSO-Wavelet Neural Network (WNN), and PSO-Elman Neural Network (ENN). AI hybrid techniques have also gained enormous attention for applications in water treatment [15,16,22].

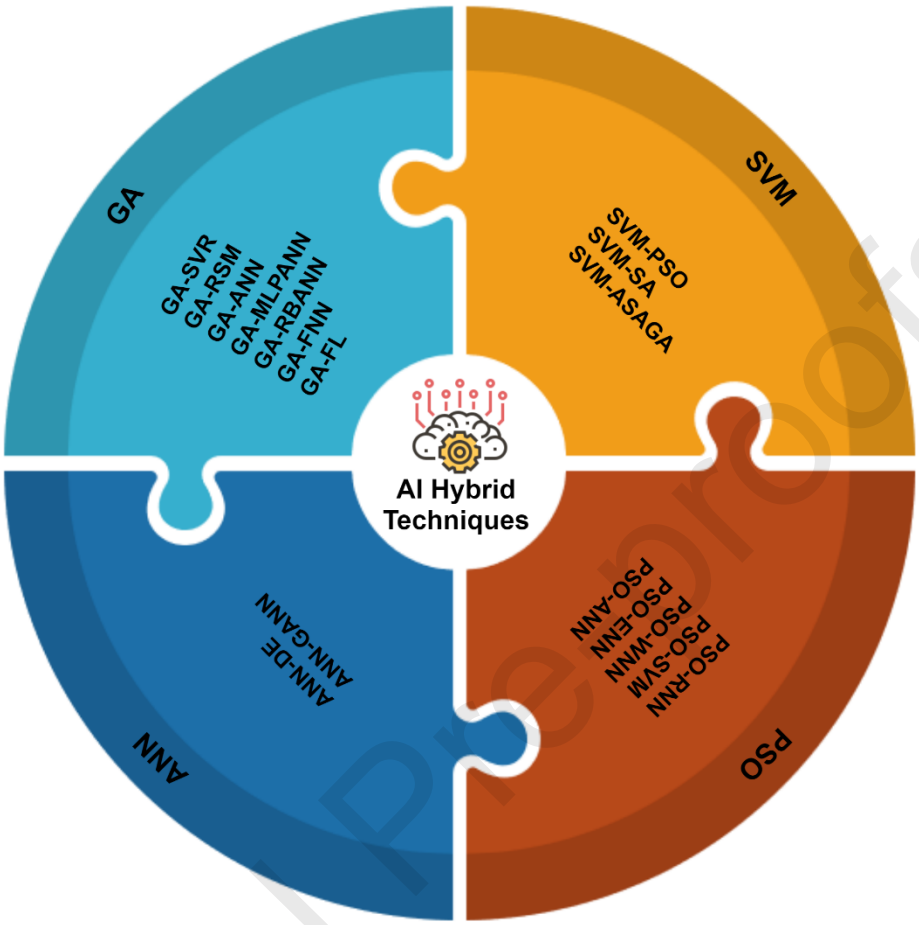

Fig. 1. AI hybrid techniques

3. Applications of AI tools in water treatment

Various studies reported the applications of AI techniques for the modelling and optimization of the water treatment process, such as pollutants removal from water. **Tables 3-5** summarizes the commonly used AI techniques employed for the adsorptive removal of metals, dyes, organic compounds, nutrients, pharmaceuticals, drugs, pesticides, and PCPs from the water.

AI techniques were effective in establishing a relationship between variables in water treatment. For example, in the adsorption of pollutants, the commonly used input variables are the initial

concentration of the pollutant, adsorbent dosage, time, pH, agitation rate and temperature, while the output variable is mainly the removal efficiency (%) and the adsorption capacity [34]. The results predicted from the models are validated using R^2 (coefficient of determination), MSE (mean squared error), SSE (sum of squared error) and RMSE (root-mean-square error) values. In most cases, the model results were in close agreement with the experimental results.

Some studies also predicted the simultaneous removal of multi-pollutants from the water with the aid of AI [35]. These findings suggest the potential applications of AI in improving the efficiency of real water treatment systems. Beside batch adsorption, AI techniques can also be employed to predict the removal performance of the adsorbents in column studies [36,37].

3.1. Removal of dyes

Several studies reported the application of AI models to predict and validate the adsorption performance of various adsorbents for the removal of dyes (**Table 2**). Most of the studies reported the removal of a single dye; however, some researchers also studied the removal of multiple dyes [38–41]. Likewise, tough simulated wastewater is used in most cases, some researchers employed real textile wastewater to evaluate the performance of the adsorbent and the model used. The R^2 values, in most cases, were greater than 0.99 that suggest the applicability of AI in evaluating the performance of the adsorption process.

The removal of methyl orange (MO), crystal violet (CV), methylene blue (MB), sunset yellow (SY), malachite green (MG), eosin yellow (EY), auramine O (AO), brilliant green (BG), eosin B (EB), acid yellow 41 (AY41), and acid red 57 (AR57) using various adsorbents was successfully modelled using the ANN, and the adsorption capacity was in close agreement with the experimental values [38–47]. The ANN models were also useful to predict the adsorption

performance of the adsorbent for the simultaneous uptake of dyes in a binary and multi-dye system [41,47–49].

3.2. Removal of heavy metals

The application of AI techniques for evaluating the removal of heavy metals using various adsorbents is presented in **Table 3**. Although some researchers reported the simultaneous adsorption of multiple metals from the aqueous phase, most of the studies are focused on single metal adsorption [50,51]. The typical inputs variables were pH, adsorbent dosage, initial metal concentration, contact time and temperature. In column studies, the effect of internal column diameter, flow rate, bed depth of column was also evaluated in addition to the above parameters [52].

The adsorption performance of different adsorbents for the removal of Cr(III), Cr(IV), Cu(II), Pb(II), As(III), Zn(II), Cd(II), and Hg(II) by different adsorbents was determined by the using various AI tools, mainly ANN [53–61] Some studies also employed the AI tools to assess the performance of adsorption for the simultaneous removal of multiple metals from aqueous phase [62] 13]. Studies also evaluated the performance of various adsorbents for the removal of dyes in a continuous system using AI tools [63].

3.3. Removal of organic compounds, nutrients, pharmaceuticals, drugs, pesticides, and PCPs from the aqueous phase

Table 4 summarizes the applications of AI tools for the removal of organic compounds, nutrients, pharmaceuticals, drugs, pesticides, and PCPs from the aqueous phase [64–68]. ANN was the commonly used model to predict the performance evaluation of the adsorption of these

pollutants. A comparison of the experimental and modelling results suggested that the AI models can safely predict the adsorption capacity or removal efficiency of the adsorbents. The commonly studied organic compounds, nutrients, pharmaceuticals, drugs, pesticides, and PCPs are cephalexin, chlorothalonil pesticide, heptachlor, triamterene, chlorophenol (CP), paracetamol, phenol, and phosphate [64,65,67,69–73]. Besides batch experiments, the performance of various column studies was also evaluated using AI tools [74].

The proposed ANN model for the adsorption of MB [75], metals (Pb(II) and Cu(II)) [77], and phenol and 3-amino-phenol [76] is presented in **Fig. 12 (a-c)**, while **Fig. 12d** represents the hybrid architecture (ANN-DE) topology employed to assess zinc removal by activated carbon [78]. The significant parameters that affect the removal process were used as input variables, while the removal efficiency was the output.

The predicted data versus experimental results for training and testing data for the adsorption of dyes is presented in **Fig. 13 (a, b**) [46]. It is evident from the experimental figure data used and the predicted results obtained by the best ANN model are in close agreement. Likewise, **Fig. 13c** compares the predicted values generated by Box-Behnken design (BBD) and ANN the models with the experimental values. It is clear that ANN is a more efficient model and accurately estimated the experimental values [79].

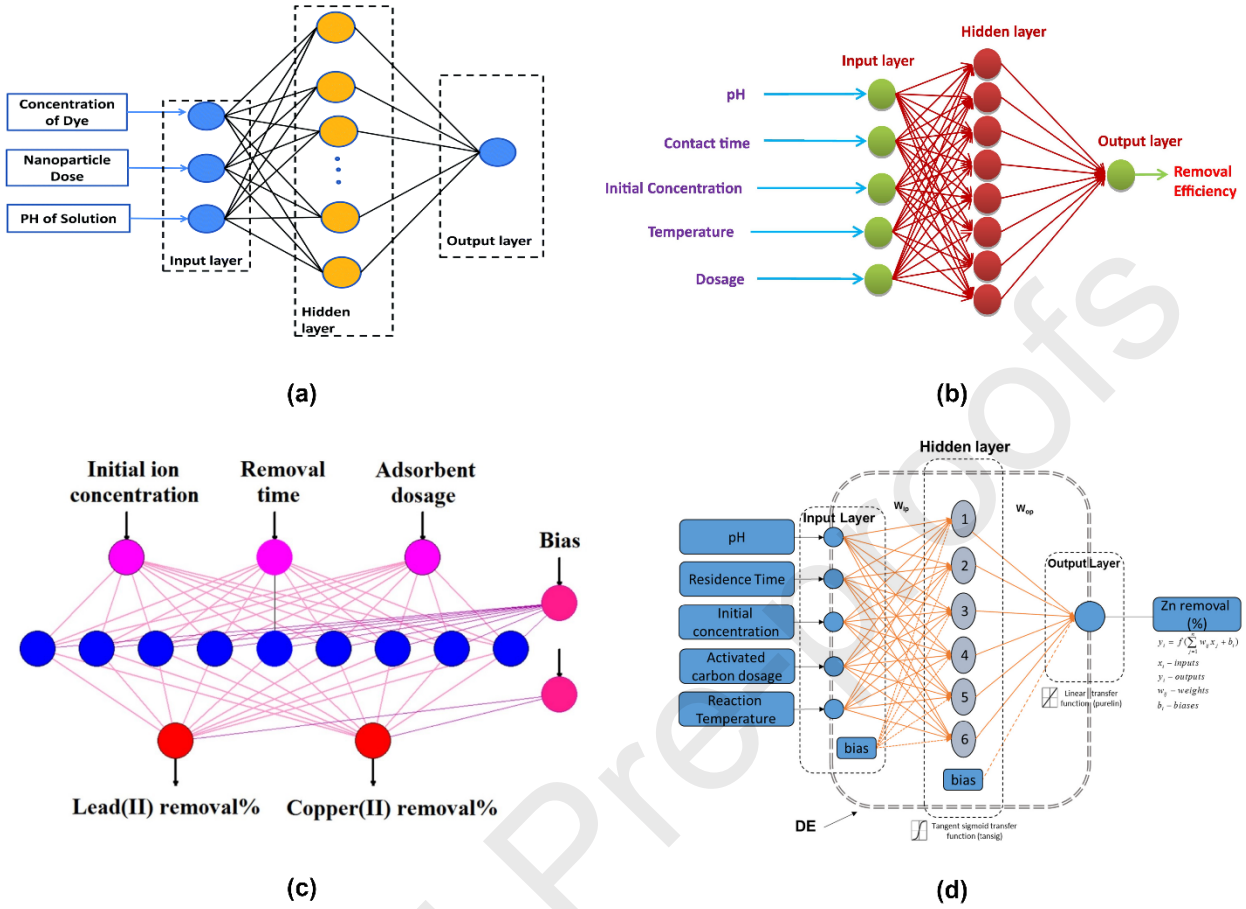

Fig. 12. Proposed ANN model for the adsorption of (a) MB. Reprinted with permission from Ref. [75]. Copyright (2020), The Royal Society of Chemistry, (b) phenol and 3-amino-phenol. Reprinted with permission from Ref. [76]. Copyright (2018), Elsevier B.V., (c) metals. Reprinted with permission from Ref. [77]. Copyright (2016), Elsevier B.V., (d) architecture of ANN-DE implementation topology. Reprinted with permission from Ref. [78]. Copyright (2018), Elsevier B.V.,

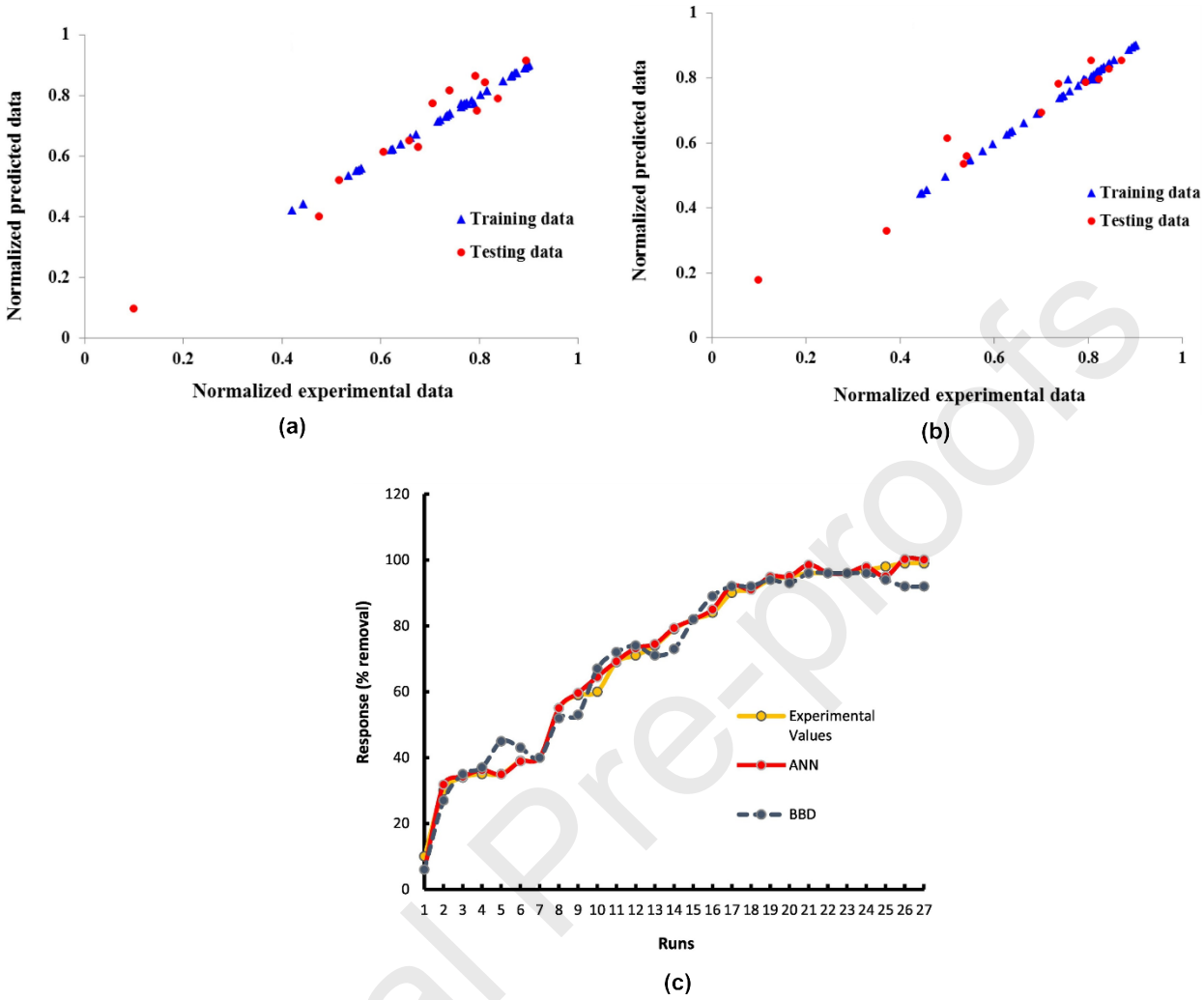

Fig. 13. A scatter plot of the ANN predicted versus experimental data of (a) BG, and (b) EB dyes simultaneous removal. Reprinted with permission from Ref. [46]. Copyright (2015), Elsevier B.V., (c) BBD and ANN predicted vs experimental data for Cu^{2+} removal. Reprinted with permission from Ref. [79]. Copyright (2018), Elsevier B.V.

3.4. Applications of hybrid techniques for the removal of pollutants

Recently AI hybrid techniques have also emerged as efficient approaches and employed extensively in water treatment for predicting the removal of various pollutants [80]. Similarly, different AI hybrids and data analytics techniques have been used for water quality analysis, process optimization, prediction, and autonomous decision making [81]. The AI hybrid

techniques reported in the literature that are employed for the removal of pollutants are MLP-ANN, ANN-GA, LS-SVM, RSM-GA, ANN-PSO, GANN, and ANN-DE, FFBP (Feed Forward Back Propagation)-ANN, BP-ANN-PSO, and PSO-GA [70,82–85] [86–91]. In general, hybrid techniques were more effective in predicting process performance as compared to individual techniques. However, still more research work needed to use the combination of different AI techniques to predict and improve the performance of various water treatment process. **Table 5** summarizes the applications of AI hybrid techniques for the removal of various pollutants from the water.

Table 2. Applications of AI for the adsorption of dyes from the aqueous phase

Dye	Adsorbent	AI technique used	Input variables	Output variable	Model validation/Performance indicators	Reference
MO	Chitosan/Al_2O_3/Fe_3O_4 core-shell composite microsphere	ANN	Time and initial concentration of MO	Adsorption capacity	R^2 = 0.998, MSE = 101.67	[38]
CV	Magnetic activated carbon (AC)	ANN	Amount of magnetic AC (MAC), pH, initial dye concentration, time, and temperature	Adsorption efficiency	R^2 = 0.9980, mean absolute percentage error (MAPE) = 0.38%	[39]
MB	Ultrasound-modified chitin (UM-chitin)	ANN	Initial concentration, temperature	Adsorption capacity	MSE < 0.0003 and R > 0.9995	[40]
SY	Nickel sulfide nanoparticle loaded on AC	ANN	Contact time, adsorbent dosage, initial dye concentration, and pH	Adsorption capacity	R^2 = 0.99 MSE =0.0003	[42]
MG	Copper nanowires loaded on AC	ANN, GA	Contact time, adsorbent dosage, initial dye concentration, and pH	Adsorption capacity	R^2 = 0.9658 MSE =0.0017	[43]
SY	AC prepared from the wood of the orange tree	ANN	Initial dye concentration, pH, adsorbent dosage, temperature, and	Removal efficiency	R^2 = 0.9966 MSE = 0.0001	[44]

			sonication time			
AR57	Mesoporous carbon-coated monolith	ANN	pH, initial dye concentration, and contact time	Removal efficiency	R^2 = 0.997, MSE = 0.9365–6.6529	[45]
EY, CV, AO, and MB	ZnO–nanorods–AC (ZnO–NR–AC)	ANN	Dyes concentrations, sonication time, and amount of sorbent	Adsorption capacity/Removal percentage	MB: R^2 = 0.9853, MSE = 0.000683 EY: R^2 = 0.999730, MSE = 0.000014 CV: R^2 = 0.987920, MSE = 0.000656 AO: R^2 = 0.997093, MSE = 0.00011	[47]
Basic Blue 41 (BB41), Basic Red 18 (BR18), and Basic Red 46 (BR46)	NiO-MnO_2 Nanocomposite	ANN	Adsorbent dosage and initial dye concentration	Adsorption capacity	R^2 = 0.9977 (BB41) R^2 = 0.9955 (BR18) R^2 = 0.9989 (BR46)	[48]
Disulfine blue (DB), rhodamine B (RB) and Chrysoidine G	Ni doped ferric oxyhydroxide FeO(OH) nanowires on AC (Ni doped FeO(OH)-NWs–AC)	ANN, RSM	Initial dye concentration, sonication time, adsorbent mass,	Adsorption capacity	CG:	[49]

(CG)			and pH		R^2 = 0.9997, MSE = 0.0055 RB: R^2 = 0.9999, MSE = 0.0033 DB R^2 = 0. 9996, MSE = 0.0046	
MB and CV	Zinc(II) oxide nanorods loaded on AC (ZnO-NRs-AC)	ANN, RSM	Adsorbent dosage, concentration, and ultrasonic time	Adsorption capacity	R^2 = 0.9999 MSE= 0.0753	[92]
Phenol red	Gold and titanium dioxide nanoparticles loaded on AC	ANN	pH, dye concentration, sorbent dosage and contact time	Removal efficiency	Au-NP-AC: R^2 = 0.9994, MSE = 5.66e-05 TiO_2-NP-AC: R^2 = 0.9729, MSE = 0.0022	[93]
SY	Zinc oxide nanorods loaded on AC	ANN	Initial dye concentration, pH, contact time, and adsorbent amount	Removal efficiency	R^2 = 0.998, MSE = 0.0008	[94]
MB	Activated spent tea (AST)	ANN	Time, adsorbent dosage, initial dye concentration, temperature, and	Adsorption efficiency	R^2 = 0.999	[95]

			pH			
Congo Red (CR)	Fe_2O_3 nanoparticles	ANN	Reaction temperature, adsorbent dose, initial dye concentration, and pH	Adsorption capacity	R^2 = 0.991, MSE = 0.00235	[96]
CV	ZnO-NR-AC	ANN	Sonication time, adsorbent doses, pH, and initial concentration	Adsorption capacity/Removal efficiency	R^2 = 0.9815, MSE = 0.000014	[97]
Basic Red (BR)	Walnut husk (WH)	ANN	Temperature, contact time, initial dye concentration, adsorbent particle size, and pH	Removal efficiency	R^2 = 0.9991, SSE = 0.2303	[98]
Ethidium bromide (EtBr)	Natural pumice and iron-coated pumice	ANN	Contact time, pH, initial EtBr concentration, and adsorbent dose	Adsorption capacity/Removal efficiency	R^2 = 0.9998, MSE = 0.005	[99]
Methyl violet 2B	Soya bean waste	ANN	pH, dosage, contact time, initial dye concentration, temperature, and ionic strength	Adsorption capacity	R^2 = 0.9946	[100]
SY	Neodymium modified ordered mesoporous carbon	ANN	Adsorbent dosage, reaction time, and initial concentration	Removal efficiency	R^2 = 0.9832 MSE = 0.0012	[101]

CV	Activated carbon prepared from *Raphia hookeri* seeds	ANN	pH, solution temperature, time, and adsorbent dosage	Adsorption capacity	R^2 = 0.9950 RMSE = 0.912	[102]
EY and MG	Monoliths HKUST-1 MOF	ANN	Sonication time, pH, adsorbent mass, and initial dye concentration	Removal efficiency	MG: R^2 = 0.9974 MSE=1.75×10^{-5} EY: R^2 = 0.9963 MSE= 7.43×10^{-5}	[103]
CG	Copper sulfide nanoparticles loaded on AC	RF	Initial dye concentration, adsorbent amount, and sonication time	Adsorption capacity	R^2 = 0.9657 MSE= 0.0021	[104]

Table 2. Applications of AI for the adsorption of heavy metals from the aqueous phase

Metal	Adsorbent	AI technique used	Input variables	Output variable	Model validation/Performance indicators	Reference
Ni(II) and Co(II)	Ultrasound-modified chitin (UM-chitin)	ANN	Initial concentration, temperature	Adsorption capacity	MSE < 0.0003 and R > 0.9995	[40]
Pb(II), Ni(II) and Cu(II)	Date seed derived biochar	ANN	Temperature, initial concentration, ionic strength, solution pH, and contact time	Adsorption capacity	R^2 = 0.9923, MSE = 1.21	[50]
Cd(II)	Immobilized *Bacillus subtilis* beads	ANN	Mass of the biosorbent, column internal diameter, flow rate, bed depth and influent concentration of metal ions	Removal efficiency	R^2 = 0.99 RMSE = 0.2289	[52]
Cu(II)	Pumice	ANN	Contact time, adsorbent dosage, initial pH, and temperature	Removal efficiency	R^2 = 0.999 RMSE = 1.122×10^{-5}	[53]
Cr(III)	Commercial Resins	ANN	pH, adsorbent dosage, initial metal concentration, contact time, and temperature	Removal efficiency	R^2 = 0.99 MSE = 0.006162	[54]
Cr(VI)	Clay-based adsorbents	ANFIS (Adaptive network based	Contact time, temperature, metal	Removal efficiency	Clay/Fe_3O_4	[55]

		fuzzy inference system)	concentration, pH, and adsorbent dose		$R^2 = 0.9997$ MSE= 1.288E-^{06}	
Cu(II)	*Gundelia tournefortii* (GT)	ANN	Temperature, initial concentration, pH, contact time, and adsorbent dosage	Biosorption capacity	$R^2 = 0.995$ MSE = 1.6868×10^{-6}	[56]
Cu(II)	Sugar beet shreds	ANN	pH of the inlet solution, initial concentration of Cu(II) ions, and adsorbent dose	Adsorption capacity	Sum of squared errors (SSer) =7.8×10^{-4} R^2 =0.9998	[57]
Pb(II)	Carboxylate-functionalized walnut shell (CFWS)	ANN	Contact time, adsorbent dosage, initial concentration, and pH	Adsorption efficiency	R^2 =0.9915	[58]
As(III)	Bacillus thuringiensis strain WS3	ANN	Contact time, As(III) concentration, temperature, pH, and adsorbent dosage	Adsorption capacity	$R^2 = 0.9959$ MSE= 0.3462	[59]
Cd(II)	*Spirulina (Arthospira) Platensis, Spirulina (Arthospira) indica,* and *Spirulina (Arthrospira) maxima*	ANN	pH, agitation speed, biosorbant dosage, and initial concentration	Removal efficiency	$R^2 = 0.965$ (*Spirulina (Arthospira) maxima*) $R^2 = 0.967$ (*Spirulina (Arthospira) platensis* $R^2 = 0.9955$ (*Spirulina (Arthospira) indica*	[60]
Hg(II)	*Sargassum Bevanom* algae	ANN	Sorbent dose, contact time, pH, and initial	Removal efficiency	R^2 =0.994	[61]

			concentration of mercury			
Cu(II), Zn(II), Ni(II) and Cd(II)	Bone char	ANN	Initial metal concentrations metals	Adsorption capacity	$R^2 > 0.96$ Modeling error = 8.01 to 45.8%	[62]
Zn(II)	*Pongamia* oil cake (*Pongamia pinnata*)	ANN	Batch: Adsorbent dosage temperature, and pH Continuous mode: Bed height, Zn(II) concentration, and flowrate	Removal efficiency	Batch: R = 0.994 MSE = 0.02275 Continuous mode: R = 0.994 MSE = 0.001216	[63]
Pb(II) and Cu(II)	Nanocomposites of rice straw and Fe_3O_4 nanoparticles	ANN	Removal time, initial ion concentration, and adsorbent dosage	Removal efficiency	Pb(II): $R^2 = 0.9905$ RMSE = 0.95 Cu(II): $R^2 = 0.9632$ RMSE= 1.87	[77]
Cu(II)	Pottery sludge	ANN	pH, initial Cu(II) concentration, contact time, and temperature	Removal percentage	MSE = 0.06819	[79]
Cd(II) and Co(II)	ZnO-NRs-AC	ANN	Adsorbent dosage, dye concentrations, and ultrasonic	Adsorption capacity	$R^2 = 0.$ 0.9999 MSE= 0.0753	[92]

			time			
Fe(III)	Ignimbrite	ANN	Particle size, flow rate, bed depth, initial concentration of Fe(III), sorption time, and pH	Adsorption capacity	$R^2 = 0.980$ RMSE= 0.65	[105]
Zn(II), Cu(II)	Bone char	ANN	Operating time, bed length, feed flow, feed concentration, ionic radius, electronegativity, and molecular weight	$C_{t,i}/C_{0,i}$ of the breakthrough curve	$R^2 > 0.99$ Mean error = 0.98 to 174%	[106]
Pb(II)	Deep eutectic solvents functionalized CNTs	ANN	Initial Pb(II) concentration, contact time, adsorbent dosage, and pH	Removal efficiency	$R^2 = 0.9956$ MSE = 1.66×10^{-4}	[107]
Pb(II)	Copper oxide nanoparticle-loaded AC (CuO-NP-AC)	ANN	Irradiation time, amount of adsorbent and ultrasound, pH, and Pb(II) ions concentration	Removal efficiency	$R^2 = 0.99970$ MSE = 0.00098	[108]
Cr(VI)	NiO nanoparticles	ANN	pH, contact time, amount of adsorbent, and initial Cr(VI) concertation	Removal efficiency	$R^2 = 0.93$	[109]

Co(II) and Ni(II)	Carboxymethyl chitosan-bounded Fe_3O_4 nanoparticles	ANN	Adsorbent mass, initial concentration of metal ions, contact time, and pH	Adsorption capacity	Ni(II): R^2 = 0.9702 MSE = 4.3256 Co(II): R^2 = 0.9673 MSE = 4.4664	[110]
Ni(II), Pb(II), and Cd(II)	Itaconic acid grafted poly(vinyl) alcohol encapsulated wood pulp (IA-g-PVA-en-WP)	ANN	Contact time, biosorbent dose, and metal concentration	Removal efficiency	R^2 = 0.997 (Cd(II)), 0.998 (Pb(II)), and 0.995 (Ni(II)) MSE = 0.003479377 (Cd(II)), 0.003830969 (Pb(II)), and 0.002372617 (Ni(II))	[111]
Pb(II)	*Gundelia tournefortii*	ANN	Contact time, biosorbent dosage, initial pH, and temperature, and initial Pb(II) ion concentration	Adsorption capacity	R^2= 0.998 MSE = 0.000867 MRE = 0.000501	[112]
As(III) and As(V)	*Botryococcus braunii*	ANN	Initial arsenic concentration, contact time, inoculum size (%v/v), and pH	Removal efficiency	As(III): R^2 = 0.9998 MSE = 2.859E $^{-05}$ As(V): R^2 = 0.9984 MSE = 1.697E $^{-05}$	[113]

Pb(II)	Coffee grounds	ANN	pH values	Adsorption capacity	$R^2 = 0.97$	[114]
Cr(VI)	Magnetic Calcium Ferrite nanoparticles ($CaFe_2O_4$)	ANN	Contact time, initial Cr(VI) ion concentration, adsorbent dosage, and pH	Adsorption capacity	$R^2 = 0.984$ MSE = 0.00161	[115]
Zn(II)	Hazelnut shell	ANN	Adsorbent dosage, initial concentration, temperature, contact time and initial pH	Adsorption capacity	$R^2 = 1$ RMSE=0.0029	[116]
Pb(II)	Rice wastes, hyacinth roots, neem leaves and coconut shells	ANN	Contact time, adsorbent dosages, initial Pb(II) ion concentration, and Initial pH	Removal efficiency	MSE = 2.186620 R = 0.985341	[117]
Cu(II)	Flax meal (oil extraction with supercritical CO_2)	ANN	Solution pH, biosorbent dosage, and metal ions concentration	Biosorption efficiency	$R^2 = 0.96$, MSE = 6.1×10^{-4}	[118]
Cd(II)	Rice straw	ANN, ANFIS	pH, initial concentration of Cd(II), and biosorbent dose	Biosorption efficiency	ANN R = 0.99 MSE=92.43	[119]
Cr(VI)	Cerium oxide polyaniline composite (CeO_2/PANI)	ANN	Initial concentration, adsorbent dose, contact time, pH, and temperature	Removal percentage	$R^2 = 0.9943$ MSE = 0.012 RMSE =0.009 MAPE = 0.016	[120]

					AARE = 0.013	
Arsenic(V)	Adsorbents obtained from the *Opuntia ficus indica* biomass	ANN	pH and temperature	Removal efficiency	R^2 = 0.9973 Modeling error (%) =2.54	[121]
Indium(III)	AC, multiwalled carbon nanotubes (MWCNTs) functionalized with OH (MWCNT–OH), and MWCNTs functionalized with COOH (MWCNT–COOH)	ANN, ANIFS	Adsorbent type, contact time, and adsorbent dosage	Adsorption capacity	ANFIS: R = 0.9998, RMSE = 48,373 ANN: R = 0.9831 MSE = 0.0180	[122]
Cr(VI)	Date palm fiber	ANN	Time, biosorbent dosage, initial concentration of Cr(VI), and initial pH	Removal efficiency	R^2 = 0.9983 MSE = 6.82	[123]
Cu(II)	Sawdust from Melia Azedarach wood	ANN, ANFIS	Adsorbent dosage, contact time, pH, and initial Cu(II) concentration	Removal efficiency	ANN: R^2 = 0.98 MSE= 10.63 ANFIS: R^2 = 0.99 MSE= 0.707	[124]
Cr(III)	Clay	ANN	Contact time, initial ion concentration, initial solution pH,	Removal efficiency	R^2 = 0.9834 MSE= 0.0247	[125]

			and adsorbent dosage			
Pb(II)	Rice husks treated with nitric acid	ANN, feed forward back-propagation neural network (FFBPNN), Levenberg–Marquardt (L–M)	Contact time, the initial concentration, and the utilized biosorbent mass	Adsorption capacity	$R^2 \approx 0.998$	[126]
Zn(II)	Rice husks digested with nitric acid	ANN	Initial concentration, contact time and temperature	Adsorption capacity	$R^2 \approx 0.9686$	[127]
Cd(II)	Nano-magnetic walnut shell-rice husk	ANN	Walnut shell-rice husk mixing ratio and magnetite loading, calcination time, and calcination temperature	Sorption efficiency	$R^2 = 0.9967$	[128]
Cu(II)	Biochar derived from rambutan (*Nephelium lappaceum*) peel	ANN, ANFIS	Initial Cu(II) ion concentration, biochar dosage, operating temperature, and contact time	Adsorption efficiency	ANFIS $R^2 = 0.9024$ RMSE = 3.29	[129]
Pb(II) and Co(II)	Rafsanjan pistachio shell (RPS)	FFNN and genetic programming (GP)	pH, Initial concentration of metal, biosorbent dosage, and temperature	Adsorption capacity	FFNN: $R^2 = 0.9932$ (Pb(II), and 0.9908 (Co(II)) RMSE = 1.1622 (Pb(II)), RMSE = 1.1340 (Co(II))	[130]

Table 4. Applications of AI for the adsorption of organic compounds, pharmaceuticals, drugs, pesticides, and PCPs from the aqueous phase

Pollutant	**Adsorbent**	**AI technique used**	**Input variables**	**Output variable**	**Model validation/Performance indicators**	**Reference**
Cephalexin	Octenyl Succinic Anhydride (OSA) starch	ANFIS	Temperature, initial concentration of adsorbent, pH, and contact time	Adsorption capacity	$R^2 = 0.9999$ RMSE= 3.9×10^{-3}	[64]
Chlorothalonil pesticide	Activated carbon	ANN	pH, chlorothalonil concentration, contact time, and adsorbent dosage	Adsorption capacity	$R^2= 0.982$ MSE=33.9	[65]
Bisphenol A (BPA), carbamazepine (CBZ), ketoprofen (KTF) and tonalide (TND)	Cross-linked chitosan/zeolite	ANN	pH and micropollutants (MP) concentration	Removal efficiency	BPA: $R^2 = 0.998$ MSE= 6.91 CBZ: $R^2 = 0.993$ MSE= 12.89 KTF: $R^2 = 0.997$ MSE= 8.20 TND: $R^2 = 0.997$	[66]

					MSE= 10.62	
Paracetamol	Chemically modified orange peel	ANN	Contact time, temperature, and initial concentration	Adsorption efficiency	MSE=5.8985 × 10^{-04} RMSE=0.0243 R^2=0.9958	[67]
Phosphate	Nanoscale zero-valent iron (nZVI)	ANN	Reaction time, stirring rate, nZVI dosage, initial PO_4^{3-} concentration, and pH	Removal efficiency	R^2 = 0.976 MSE=1.84	[68]
Heptachlor	Fe/Cu nanoparticles	ANN	Adsorbent dose, pH, initial heptachlor concentration, stirring rate, and contact time	Removal efficiency	R^2= 0.9567 MSE =21.0248	[69]
Triamterene	MWCNTs and single-walled carbon nanotubes (SWCNTs)	ANN	Contact time, initial drug concentration, amount of adsorbent, and temperature	Adsorption capacity/ Removal efficiency	R^2 = 0.980 MSE= 0.002	[70]
Chlorophenol (CP)	Coconut shell carbon (CSC)	Radial basis function network (RBFN) and multilayer perceptron network (MLPN)	Contact time, CP concentration, temperature, and pH	Removal efficiency	RBFN: R^2 = 0.96 MSE= 6.03	[71]
Phenol	Scoria stone	ANN	Phenol concentration, contact time, and adsorbent dosage	Removal efficiency	R^2 =0.982686 RMSE= 2.464535	[72]
Phosphate	Lime-iron sludge	ANN and ANFIS	Time, flow rate, and bed depth	Breakthrough time and Concentration ratio (C_t/C_o)	C_t/C_o = R^2 = 0.9962 (ANFIS) R^2 = 0.9968 (ANN)	[73]

					Breakthrough times: $R^2 = 1$ (ANFIS) $R^2 = 1$ (ANN) MSE: 0.0004 (ANN) 0.0001 (ANFIS)	
Phenol	Activated date palm biochar	ANN	Time, mass of adsorption bed, depth of adsorption bed, flow rate, and initial concentration	Residual concentration of the effluent phenol and the breakthrough C_t/C_o	$R^2 = 0.9880$ RMSE= 0.0472	[74]
Ortho-cresol	Activated date palm biochar	ANN	Time, mass of adsorption bed, depth of adsorption bed, flow rate, and initial concentration	Residual concentration of the effluent ortho-cresol and the breakthrough C_t/C_o	$R^2 = 0.9886$ RMSE= 0.0560	[74]
Phenol and 3-amino-phenol	Composite iron nano-adsorbent	ANN	Phenols concentration, pH, contact time, temperature and the quantity of sorbent	Uptake effectiveness	Relative error = ±0.35 to 3.0 for phenol and 0.35 to 3.5 for *p*-amino-phenol	[76]
Carbaryl	*Lemna major* biomass	ANN	Initial concentration, pH, biomass dose and contact time	Adsorption capacity	$R^2 = 0.921$	[131]
Nimesulide and paracetamol	AC	ANN	Contact time, adsorbent dose, adsorbent particle size, and initial concentration	Adsorption capacity	$R^2 = 0.9989$ (imesulide) (paracetamol) ($R^2 = 0.9985$) *MSE* = 0.0006	[132]

Ranitidine hydrochloride (RH)	Mung bean husk (MBH)	ANN	Adsorbent dose, pH, and agitation	Adsorption efficiency	R^2 = 0.9821 RMSE = 0.2292	[133]
Phenol and resorcinol	AC, wood charcoal (WC) and rice husk ash (RHA).	ANN	pH, contact time, initial concentrations of phenol and resorcinol, and amount of adsorbent	Removal efficiency	Phenol: R^2 = 0.96 RMSE = 2.4 Resorcinol: R^2 = 0.95 RMSE = 4.5	[134]
Phenol	AC	ANN	pH, contact time, temperature, initial concentration of phenol, and amount of adsorbent	Adsorption capacity/ Removal efficiency	R^2 = 0.9998 RMSE = 0.2378	[135]
Phenol	Orange peel ash	ANN	Temperature, stirring rate, contact time, adsorbents dose, pH, and initial concentration	Uptake efficiency	MSE = 0.0006	[136]
Benzene, toluene, ethyl benzene and xylene (BTEX)	Iron nanoparticles	ANN	pH, temperature, adsorbent dose, initial BTEX mixture concentration, and contact time	Removal efficiency	R^2 = 0.97064 MSE: 0.080186	[137]
Phosphate	Hydrated ferric oxide-based nanocomposite	ANN	Adsorbent dosage, operating temperature, sulfate concentration, and initial pH	Removal efficiency	R^2 = 0.9931 MSE= 0.00105	[138]

Table 5. Applications of AI hybrid techniques for the adsorption of pollutants from the aqueous phase

Pollutant	**Adsorbent**	**AI technique used**	**Input variable**	**Output variable**	**Model validation/ performance indicators**	**Reference**
AY41 and SY	SnO_2 nanoparticle loaded activated carbon	(Principal component analysis) PCA- ANN	Dye concentration, pH, adsorbent dosage, and contact time	Removal efficiency	SY: $R^2 = 0.99$ MSE = 0.53 AY41: $R^2 = 0.98$ MSE = 0.79	[41]
BG and EB	ZnS nanoparticles loaded AC	Multi-layer ANN (ML-ANN), RSM	Contact time, adsorbent dosage, BG concentration, EB concentration	Adsorption capacity	BG: $R^2 = 0.9589$, MSE = 0.0021 EB: $R^2 = 0.9455$, MSE = 0.0022	[46]
Metals (Cd, Al, Co, Cu, Fe, and Pb)	Chitosan and Chitosan-Montmorillonite nanocomposite	Multi-layer perceptron ANN (MLP-ANN), radial basis function ANN (ANN-RBF), SOS algorithm (ANN–	Adsorbent dosage, initial pH values, and contact time	Removal efficiency	Chitosan: $R^2 = 0.9527$ (MLPANN), 0.9643 (RBFANN) C. M. Nanocomposite:	[51]

		SOS)			R^2 = 0.9257 (MLPANN), 0.9665 (RBFANN)	
MG	Chitosan/polyvinyl alcohol/zeolite imidazolate frameworks membrane adsorbents (CPZ)	MLP-ANN	pH, initial dye concentration, and adsorbent dose	Removal efficiency	R^2 = 0.9958 RMSE = 0.01822	[81]
As(III)	Cerium oxide tetraethylenepentamine (CTEPA)	GP (genetic programming), LS-SVM (least square support vector machine)	Temperature, time, concentration, pH and dose	Adsorption capacity	GP: R^2 = 0.977 MSE = 0.1068 RMSE = 0.0284 MAPE (mean absolute percentage error) = 0.0632 AARE (average absolute relative error) = 0.0004 LS-SVM: R^2 = 0.905 MSE =1.423 RMSE = 0.112 MAPE = 0.200 AARE = 0.002	[86]

Cr(VI)	Cupric oxide nanoparticles (CuONPs)	ANN-GA	Initial concentration, pH, adsorbent dose, and temperature	Removal percentage	R^2 = 0.99 MSE = 0.21	[87]
As(III)	Zn-loaded pinecone biochar	RSM-GA (response surface model–genetic algorithm)	As(III) concentration, EtOH concentration, and pH	Adsorption capacity	R^2 = 0.92-0.95 RMSE = 0.28-0.25 SEP (standard error of prediction) = 3.17-2.80	[88]
Cu(II)	Reduced graphene oxide-supported nanoscale zero-valent iron (nZVI/rGO) magnetic nanocomposites	ANN-GA, ANN-PSO	Temperature, initial pH, initial concentration and contact time	Removal efficiency	R^2 = 0.9997 MSE = 0.00020	[89]
Cd(II)	Natural waste materials (leaves of jackfruit, mango and rubber plants)	GA-ANN	Number of sorbent, pH, adsorbent dosage, time, and initial concentration	Removal efficiency	R = 0.97–0.99 MSE = 0.98-12.16	[91]
MB	Zinc sulfide nanoparticles with AC (ZnS-NPs-AC)	LS-SVM (least squares-support vector machine), ANN, GA	Sonication time, MB concentration, adsorbent mass, and pH	Adsorption capacity	ANN: R^2 = 0.9984, RMSE = 0.00065	[139]

Basic Red 18 (BR 18) and Basic Blue 41(BB 41)	CuO–NiO nanocomposite	ANN, BP-ANN (backpropagation neural network)	Dye concentration and adsorbent dosage	Removal efficiency	R^2 = 0.9904 (BR 18) R^2 = 0.9964 ((BB41)	[140]
Acid red 27	Polypyrrole/$SrFe_{12}O_{19}$/graphene oxide nanocomposite	ANN-BA (bees-inspired algorithm) MLP-ANN (multilayer perceptron artificial neural networks)	Contact time, shaking rate, initial concentration, pH, and adsorbent dosage	Adsorption efficiency	-	[141]
MB	Sulfur–nitrogen co-doped Fe_2O_3 nanostructure surface	ANN-GA	Dye concentration, the light dose, pH, and dose of the nanoparticle	Removal efficiency	R^2 = 0.92	[142]
MB	Mesoporous rGO/Fe/Co nanohybrids	ANN-PSO, ANN-GA	Initial concentration, contact time, temperature, and pH	Adsorption capacity	Absolute error = 0.52	[143]
CV	Reduced-graphene-oxide-supported bimetallic Fe/Ni nanoparticles (rGO/Fe/Ni)	ANN-GA, ANN-PSO, and BBD (Box Behnken design)	Initial dye concentration, initial pH, contact time, and temperature	Removal efficiency	R^2 = 0.9998 (BP-ANN) Absolute errors: 5.6 (ANN-GA) 3.5 (ANN-PSO) 12.4 (BBD)	[144]

Zn(II)	Activated carbon derived from palm oil kernel shell	Differential evolution (DEO) embedded neural network (ANN-DE)	Initial solution concentration, pH, adsorbent dosage, residence time, temperature	Removal efficiency	R^2 = 0.995 RMSE = 0.248	[78]
Cd(II)	Inactive and *living Trichoderma viride* biomass	SVR-GA (Support Vector Regression- genetic algorithm)	pH, biomass dosage, metal concentration, contact time and temperature	Biosorption efficiency	R^2 = 0.919 MSE = 0.85	[145]
Cr(VI)	Activated carbon from Medlar seed (Mespilus germanica)	SVR-GA	pH, initial concentration of Cr(VI), adsorbent dosage and contact time	Removal efficiency	R^2 = 0.981	[146]
Cd(II)	Biowaste materials, jackfruit, mango, and rubber leaves	GA-ANN	Adsorbent type, bed height, flow rate, time, and influent concentration	Adsorption efficiency	R = 0.997-0.999 MSE = 1.470807-4.238426	[147]

4. Challenges and Prospects

AI tools have offered serval advantages over conventional mathematical modelling. It can be used to predict the performance of various water treatment process and reduce the experimental costs. However, still, there are some limitations that hindered the widespread applications of these techniques in real water treatment.

The major drawback of AI tools such as ANNs is the poor reproducibility due to random weight and bias that might result in a locally optimal solution [16,148]. The hybridization of various AI tools can also be employed to predict pollutant removal efficiency during the adsorption process. Deep learning and deep ANNs are good options for achieving high accuracy and prediction. However, it requires a sufficient amount of data for experimental training, testing, finding the local minima and overfitting.

The process performance predicted by AI tools may also deviate from the actual results under certain circumstances. For example, a sudden change in operating parameters and water quality may result in wrong prediction by AI tools. Efforts must be made to strengthen the prediction of AI tools so that they can be employed under various circumstances and can accommodate sudden fluctuation in the input variables. Based on the available literature, the AI tools have demonstrated tremendous performance for modelling the batch adsorption process with a smaller range of data. However, the applications of AI tools in practical wastewater treatment with a wide range of data is yet to be explored.

Another major challenge relevant to AI-based water treatment is the availability and selection of data. The water utilities are acquired to generate, collect, process, evaluate and analyze data by creating datasets for system optimization and prediction. Special attention must be given to select the training data for AI tools, an experimental design technique, as the random data selection is

associated with certain drawbacks. However, the experimental design techniques (such as RSM) usually require a large input dataset to create an accurate response.

The operational data from real water treatment plants can be used as input for AI models, and the removal of pollutants can be predicted more accurately. AI technology could play a critical role in sustainable wastewater treatment and can result in a significant reduction in operating cost in addition to safeguarding the environment. Besides predicting the water treatment process efficiency, AI tools can be used to integrate the whole process of water treatment starting from water discharge, transportation, management of sludge, environmental impacts, economy and policymaking. Data collection from the various water treatment process is necessary to apply AI techniques in the water treatment domain successfully. However, special care should be taken while collecting the data to keep data integrity. All the information, such as data sources, location, process environment, and dataset ontology, should be listed while reporting the data. This information will help researchers, students, and engineers to reuse the data in the various experimental domain for future prediction.

AI provides an opportunity for the water industry to optimize and govern water monitoring and management. The development of new AI-based algorithms is needed to address certain problems in water treatment and management, such as water quality, leakage detection, and water process optimization, to provide intelligent decisions. By applying hybrid AI techniques, prediction accuracy can be enhanced that leads to a reduction in energy and operational cost.

A benchmark/framework should be developed to compare various AI-based stand-alone and hybrid techniques in the field of water treatment and to suggest the best techniques for applications in real treatment processes.

5. Conclusion

AI has transformative potentials to revolutionize the wastewater treatment process. This review summarized the major AI tools employed in water treatment for the uptake of various pollutants. Numerous AI models (both single and hybrid) have successfully predicted the performance of different adsorbents for the removal of dyes, metals, organic compounds, pharmaceuticals, drugs, pesticides and PCPs from water. Despite several advantages offered by AI tools, there are still some shortcoming that needs to be overcome to fully utilize the potential of AI tools in practical water treatment applications. Selection of suitable data, applications of hybrid AI tools, and more studies at the pilot plant level will be helpful to address these challenges. Regardless of these hurdles, the current research progress suggests that AI tools have a bright future in water treatment applications.

Appendix:

List of abbreviations

SDGs: Sustainable Development Goals

PCPs: Personal Care Products

AI: Artificial Intelligence

ANN: Artificial Neural Network

DT: Decision Tree

MLP: Multi Layer Perceptron

BP: Back Propagation

ANFIS: Adaptive Network based Fuzzy Inference System

RSM: Response Surface Methodology

RBF: Radial Basis Function

CNN: Convoluted Neural Network

PSO: Particle Swarm Optimization

GA: Genetic Algorithm

RF: Random Forest

KNNs: k-Nearest Neighbor

SVM: Support Vector Machine

RNN: Recurrent Neural Network

SOM: Self-Organizing Map

FNN: Fuzzy Neural Network

DNN: Deep Neural Network

MLPANN: Multilayer Perceptron Artificial Neural Network

MLP: Multi Layer Perceptron

MLPN: Multilayer Perceptron Network

FFBP: Feed forward control

FFBP: Feed Forward Neural Network

RBFN: Radial Basis Function Network

GP: Genetic Programming

LM: Levenberg Marquarit

FFBPNN: Feed Forward Back Propagation Neural Network

ANN-BA: Artificial Neural Network-Bees Inspired Algorithm

LS-SVM: Least Square-Support Vector Machine

GA-SVR: Genetic Algorithm-Support Vector Regression

GA-RSM: Genetic Algorithm-Response Surface Model

GA-MLPANN: Genetic Algorithm -Multi Layer Perceptron Artificial Neural Network

GA-RBANN: Genetic Algorithm -Radial Basis Function Artificial Neural Network

GA-FNN: Genetic Algorithm -Feedforward Neural Network

GA-FL: Genetic Algorithm -Fuzzy Logic

SVM-SA: Support Vector Machine-Simulated Annealing

SVM-ASAGA: Support Vector Machine-Adaptive Simulated Annealing Genetic Algorithm

ANN-DE: Artificial Neural Network-Differential Evolution

GANN: Genetic Algorithm Neural Network

PSO-WNN: Particle Swarm Optimization-Wavelet Neural Network

PSO-ENN: Particle Swarm Optimization-Elman Neural Network

PCA- ANN: Principal Component Analysis-Artificial Neural Network

R^2: Coefficient of Determination)

MSE: Mean Squared Error

SSE: Sum of Squared Error

RMSE: Root-Mean-Square Error

MAPE: Mean Absolute Percentage Error

AARE: Average Absolute Relative Error

SEP: Standard Error of Prediction

References

[1] UN, Department of Economic and Social Affairs Sustainable Development, (2015). https://sdgs.un.org/topics/water-and-sanitation (accessed November 26, 2020).

[2] D. Cheng, H.H. Ngo, W. Guo, S.W. Chang, D.D. Nguyen, Y. Liu, Q. Wei, D. Wei, A critical review on antibiotics and hormones in swine wastewater: Water pollution problems and control approaches, J. Hazard. Mater. 387 (2020) 121682. https://doi.org/10.1016/j.jhazmat.2019.121682.

[3] B.W. Abbott, K. Bishop, J.P. Zarnetske, C. Minaudo, F.S. Chapin, S. Krause, D.M. Hannah, L. Conner, D. Ellison, S.E. Godsey, S. Plont, J. Marçais, T. Kolbe, A. Huebner, R.J. Frei, T. Hampton, S. Gu, M. Buhman, S. Sara Sayedi, O. Ursache, M. Chapin, K.D. Henderson, G. Pinay, Human domination of the global water cycle absent from depictions and perceptions, Nat. Geosci. 12 (2019) 533–540. https://doi.org/10.1038/s41561-019-0374-y.

[4] I. Ihsanullah, MXenes (two-dimensional metal carbides) as emerging nanomaterials for water purification: Progress, challenges and prospects, Chem. Eng. J. 388 (2020) 124340. https://doi.org/10.1016/j.cej.2020.124340.

[5] I. Ihsanullah, Boron nitride-based materials for water purification: Progress and outlook, Chemosphere. 263 (2020) 127970. https://doi.org/10.1016/j.chemosphere.2020.127970.

[6] M. Zubair, I. Ihsanullah, H. Abdul Aziz, M. Azmier Ahmad, M.A. Al-Harthi, Sustainable wastewater treatment by biochar/layered double hydroxide composites: Progress, challenges, and outlook, Bioresour. Technol. 319 (2020) 124128. https://doi.org/10.1016/j.biortech.2020.124128.

[7] M. Naushad, Surfactant assisted nano-composite cation exchanger: Development, characterization and applications for the removal of toxic Pb2+ from aqueous medium, Chem. Eng. J. 235 (2014) 100–108. https://doi.org/10.1016/j.cej.2013.09.013.

[8] M. Naushad, G. Sharma, Z.A. Alothman, Photodegradation of toxic dye using Gum Arabic-crosslinked-poly(acrylamide)/Ni(OH)2/FeOOH nanocomposites hydrogel, J. Clean. Prod. 241 (2019) 118263. https://doi.org/10.1016/j.jclepro.2019.118263.

[9] U. Paschen, C. Pitt, J. Kietzmann, Artificial intelligence: Building blocks and an innovation typology, Bus. Horiz. 63 (2020) 147–155. https://doi.org/10.1016/j.bushor.2019.10.004.

[10] Z. Allam, Z.A. Dhunny, On big data, artificial intelligence and smart cities, Cities. 89 (2019) 80–91. https://doi.org/10.1016/j.cities.2019.01.032.

[11] Y. Lu, Artificial intelligence: a survey on evolution, models, applications and future trends, J. Manag. Anal. 6 (2019) 1–29. https://doi.org/10.1080/23270012.2019.1570365.

[12] M. Ghahramani, Y. Qiao, M. Zhou, A.O. Hagan, J. Sweeney, AI-based modeling and data-driven evaluation for smart manufacturing processes, IEEE/CAA J. Autom. Sin. 7 (2020) 1026–1037. https://arxiv.org/abs/2008.12987.

[13] W. STAFF, Report: Data demand will drive $92 billion in investment by 2030, (2020). https://waterfm.com/report-data-demand-will-drive-92-billion-in-investment-by-2030/ (accessed November 24, 2020).

[14] W. STAFF, Report: Annual OPEX for water and wastewater utilities nearing $100 billion, (2018). https://waterfm.com/report-opex-water-wastewater-utilities-nearing-100-billion-per-year/ (accessed November 24, 2020).

[15] M. Bagheri, A. Akbari, S.A. Mirbagheri, Advanced control of membrane fouling in filtration systems using artificial intelligence and machine learning techniques: A critical review, Process Saf. Environ. Prot. 123 (2019) 229–252. https://doi.org/10.1016/j.psep.2019.01.013.

[16] L. Zhao, T. Dai, Z. Qiao, P. Sun, J. Hao, Y. Yang, Application of artificial intelligence to wastewater treatment: A bibliometric analysis and systematic review of technology, economy, management, and wastewater reuse, Process Saf. Environ. Prot. 133 (2020) 169–182. https://doi.org/10.1016/j.psep.2019.11.014.

[17] L. Jiang, Z. Cai, D. Wang, S. Jiang, Survey of improving k-nearest-neighbor for classification, in: Surv. Improv. k-Nearest-Neighbor Classif., IEEE, 2007: pp. 679–683. https://doi.org/10.1109/FSKD.2007.552.

[18] J. Han, J. Pei, M. Kamber, Data mining: concepts and techniques, Elsevier, 2012. https://doi.org/10.1016/C2009-0-61819-5.

[19] R. Genuer, J.-M. Poggi, C. Tuleau-Malot, Variable selection using random forests, Pattern Recognit. Lett. 31 (2010) 2225–2236. https://doi.org/10.1016/j.patrec.2010.03.014.

[20] I.A. Basheer, M. Hajmeer, Artificial neural networks: fundamentals, computing, design, and application, J. Microbiol. Methods. 43 (2000) 3–31. https://doi.org/10.1016/S0167-7012(00)00201-3.

[21] S. Ding, H. Li, C. Su, J. Yu, F. Jin, Evolutionary artificial neural networks: a review, Artif. Intell. Rev. 39 (2013) 251–260. https://doi.org/10.1007/s10462-011-9270-6.

[22] J.J. Buckley, H. Yoichi, Neural nets for fuzzy systems, Fuzzy Sets Syst. 71 (1995) 265–276. https://doi.org/10.1016/0165-0114(94)00282-C.

[23] I. Goodfellow, Y. Bengio, A. Courville, Y. Bengio, Deep learning, MIT press Cambridge, 2016. https://mitpress.mit.edu/books/deep-learning.

[24] Y. Pang, M. Sun, X. Jiang, X. Li, Convolution in Convolution for Network in Network, IEEE Trans. Neural Networks Learn. Syst. 29 (2018) 1587–1597. https://doi.org/10.1109/TNNLS.2017.2676130.

[25] O. Abdel-Hamid, A.-R. Mohamed, H. Jiang, L. Deng, G. Penn, D. Yu, Convolutional Neural Networks for Speech Recognition, IEEE/ACM Trans. Audio, Speech and Lang. Proc. 22 (2014) 1533–1545. https://doi.org/10.1109/TASLP.2014.2339736.

[26] J. Schmidhuber, Deep learning in neural networks: An overview, Neural Networks. 61 (2015) 85–117. https://doi.org/10.1016/j.neunet.2014.09.003.

[27] G. Pandey, A. Dukkipati, Learning by stretching deep networks, in: Proc. 31 St Int. Conf. Mach. Learn. Beijing, China, 2014: pp. 1719–1727. http://proceedings.mlr.press/v32/pandey14.pdf.

[28] C. Gao, J. Yan, S. Zhou, P.K. Varshney, H. Liu, Long short-term memory-based deep recurrent neural networks for target tracking, Inf. Sci. (Ny). 502 (2019) 279–296. https://doi.org/10.1016/j.ins.2019.06.039.

[29] B. Yekkehkhany, A. Safari, S. Homayouni, M. Hasanlou, A comparison study of different kernel functions for SVM-based classification of multi-temporal polarimetry SAR data, Int. Arch. Photogramm. Remote Sens. Spat. Inf. Sci. 40 (2014) 281–285. https://doi.org/10.5194/isprsarchives-XL-2-W3-281-2014.

[30] X. Qu, L. Yang, K. Guo, L. Ma, M. Sun, M. Ke, M. Li, A survey on the development of self-organizing maps for unsupervised intrusion detection, Mob. Networks Appl. (2019) 1–22. https://doi.org/10.1007/s11036-019-01353-0.

[31] A.H. Beg, M.Z. Islam, Advantages and limitations of genetic algorithms for clustering records, in: IEEE 11th Conf. Ind. Electron. Appl. (ICIEA), Hefei, China, 2016, IEEE, 2016: pp. 2478–2483. https://doi.org/10.1109/ICIEA.2016.7604009.

[32] T. Cura, A particle swarm optimization approach to clustering, Expert Syst. Appl. 39

(2012) 1582–1588. https://doi.org/10.1016/j.eswa.2011.07.123.

[33] J.C. Bansal, Particle swarm optimization, in: Evol. Swarm Intell. Algorithms, Springer, 2019: pp. 11–23. https://doi.org/10.1007/978-3-319-91341-4.

[34] A.M. Ghaedi, A. Vafaei, Applications of artificial neural networks for adsorption removal of dyes from aqueous solution: A review, Adv. Colloid Interface Sci. 245 (2017) 20–39. https://doi.org/10.1016/j.cis.2017.04.015.

[35] H.E. Reynel-Avila, A. Bonilla-Petriciolet, G. de la Rosa, Analysis and modeling of multicomponent sorption of heavy metals on chicken feathers using Taguchi's experimental designs and artificial neural networks, Desalin. Water Treat. 55 (2015) 1885–1899. https://doi.org/10.1080/19443994.2014.937762.

[36] L. Cavas, Z. Karabay, H. Alyuruk, H. Doğan, G.K. Demir, Thomas and artificial neural network models for the fixed-bed adsorption of methylene blue by a beach waste Posidonia oceanica (L.) dead leaves, Chem. Eng. J. 171 (2011) 557–562. https://doi.org/10.1016/j.cej.2011.04.030.

[37] B. Balci, O. Keskinkan, M. Avci, Use of BDST and an ANN model for prediction of dye adsorption efficiency of Eucalyptus camaldulensis barks in fixed-bed system, Expert Syst. Appl. 38 (2011) 949–956. https://doi.org/10.1016/j.eswa.2010.07.084.

[38] B. Tanhaei, A. Ayati, M. Lahtinen, B. Mahmoodzadeh Vaziri, M. Sillanpää, A magnetic mesoporous chitosan based core-shells biopolymer for anionic dye adsorption: Kinetic and isothermal study and application of ANN, J. Appl. Polym. Sci. 133 (2016). https://doi.org/10.1002/app.43466.

[39] I. Salehi, M. Shirani, A. Semnani, M. Hassani, S. Habibollahi, Comparative Study Between Response Surface Methodology and Artificial Neural Network for Adsorption of Crystal Violet on Magnetic Activated Carbon, Arab. J. Sci. Eng. 41 (2016) 2611–2621. https://doi.org/10.1007/s13369-016-2109-3.

[40] P.S. Pauletto, G.L. Dotto, N.P.G. Salau, Optimal artificial neural network design for simultaneous modeling of multicomponent adsorption, J. Mol. Liq. 320 (2020) 114418. https://doi.org/10.1016/j.molliq.2020.114418.

[41] S. Hajati, M. Ghaedi, Z. Mahmoudi, R. Sahraei, SnO2 nanoparticle-loaded activated carbon for simultaneous removal of Acid Yellow 41 and Sunset Yellow; derivative spectrophotometric, artificial neural network and optimization approach, Spectrochim.

Acta Part A Mol. Biomol. Spectrosc. 150 (2015) 1002–1012. https://doi.org/10.1016/j.saa.2015.06.008.

[42] M. Ghaedi, N. Zeinali, M. Maghsoudi, M.K. Purkait, Artificial Neural Network (ANN) Method for Modeling of Sunset Yellow Dye Adsorption Using Nickel Sulfide Nanoparticle Loaded on Activated Carbon: Kinetic and Isotherm Study, J. Dispers. Sci. Technol. 36 (2015) 1339–1348. https://doi.org/10.1080/01932691.2014.964359.

[43] M. Ghaedi, E. Shojaeipour, A.M. Ghaedi, R. Sahraei, Isotherm and kinetics study of malachite green adsorption onto copper nanowires loaded on activated carbon: Artificial neural network modeling and genetic algorithm optimization, Spectrochim. Acta Part A Mol. Biomol. Spectrosc. 142 (2015) 135–149. https://doi.org/10.1016/j.saa.2015.01.086.

[44] A.M. Ghaedi, M. Ghaedi, P. Karami, Comparison of ultrasonic with stirrer performance for removal of sunset yellow (SY) by activated carbon prepared from wood of orange tree: Artificial neural network modeling, Spectrochim. Acta Part A Mol. Biomol. Spectrosc. 138 (2015) 789–799. https://doi.org/10.1016/j.saa.2014.11.019.

[45] M.R. Malekbala, S. Hosseini, S. Masoudi Soltani, R. Malekbala, T.S.Y. Choong, F. Eghbali Babadi, Development, application, and evaluation of artificial neural network in investigating the removal efficiency of Acid Red 57 by synthesized mesoporous carbon-coated monoliths, Desalin. Water Treat. 56 (2015) 2246–2257. https://doi.org/10.1080/19443994.2014.959062.

[46] M. Jamshidi, M. Ghaedi, K. Dashtian, A.M. Ghaedi, S. Hajati, A. Goudarzi, E. Alipanahpour, Highly efficient simultaneous ultrasonic assisted adsorption of brilliant green and eosin B onto ZnS nanoparticles loaded activated carbon: Artificial neural network modeling and central composite design optimization, Spectrochim. Acta Part A Mol. Biomol. Spectrosc. 153 (2016) 257–267. https://doi.org/10.1016/j.saa.2015.08.024.

[47] E.A. Dil, M. Ghaedi, A.M. Ghaedi, A. Asfaram, A. Goudarzi, S. Hajati, M. Soylak, S. Agarwal, V.K. Gupta, Modeling of quaternary dyes adsorption onto ZnO–NR–AC artificial neural network: Analysis by derivative spectrophotometry, J. Ind. Eng. Chem. 34 (2016) 186–197. https://doi.org/10.1016/j.jiec.2015.11.010.

[48] N.M. Mahmoodi, Z. Hosseinabadi-Farahani, H. Chamani, Dye adsorption from single and binary systems using NiO-MnO2 nanocomposite and artificial neural network modeling, Environ. Prog. Sustain. Energy. 36 (2017) 111–119. https://doi.org/10.1002/ep.12452.

[49] F.N. Azad, M. Ghaedi, A. Asfaram, A. Jamshidi, G. Hassani, A. Goudarzi, M.H.A. Azqhandi, A. Ghaedi, Optimization of the process parameters for the adsorption of ternary dyes by Ni doped FeO (OH)-NWs–AC using response surface methodology and an artificial neural network, RSC Adv. 6 (2016) 19768–19779. https://doi.org/10.1039/C5RA26036A.

[50] A. El Hanandeh, Z. Mahdi, M.S. Imtiaz, Modelling of the adsorption of Pb, Cu and Ni ions from single and multi-component aqueous solutions by date seed derived biochar: Comparison of six machine learning approaches, Environ. Res. 192 (2021) 110338. https://doi.org/10.1016/j.envres.2020.110338.

[51] A.H. Hamidian, S. Esfandeh, Y. Zhang, M. Yang, Simulation and optimization of nanomaterials application for heavy metal removal from aqueous solutions, Inorg. Nano-Metal Chem. 49 (2019) 217–230. https://doi.org/10.1080/24701556.2019.1653321.

[52] M.F. Ahmad, S. Haydar, Evaluation of a newly developed biosorbent using packed bed column for possible application in the treatment of industrial effluents for removal of cadmium ions, J. Taiwan Inst. Chem. Eng. 62 (2016) 122–131. https://doi.org/10.1016/j.jtice.2015.12.032.

[53] N.G. Turan, B. Mesci, O. Ozgonenel, The use of artificial neural networks (ANN) for modeling of adsorption of Cu(II) from industrial leachate by pumice, Chem. Eng. J. 171 (2011) 1091–1097. https://doi.org/10.1016/j.cej.2011.05.005.

[54] A.E. Tümer, S. Edebali, Modeling of Trivalent Chromium Sorption onto Commercial Resins by Artificial Neural Network, Appl. Artif. Intell. 33 (2019) 349–360. https://doi.org/10.1080/08839514.2019.1577015.

[55] R. Foroutan, S.J. Peighambardoust, R. Mohammadi, M. Omidvar, G.A. Sorial, B. Ramavandi, Influence of chitosan and magnetic iron nanoparticles on chromium adsorption behavior of natural clay: Adaptive neuro-fuzzy inference modeling, Int. J. Biol. Macromol. 151 (2020) 355–365. https://doi.org/10.1016/j.ijbiomac.2020.02.202.

[56] S. Golshan Shandi, F. Doulati Ardejani, F. Sharifi, Assessment of Cu (II) removal from an aqueous solution by raw Gundelia tournefortii as a new low-cost biosorbent: Experiments and modelling, Chinese J. Chem. Eng. 27 (2019) 1945–1955. https://doi.org/10.1016/j.cjche.2018.12.027.

[57] N. Blagojev, D. Kukić, V. Vasić, M. Šćiban, J. Prodanović, O. Bera, A new approach for

modelling and optimization of Cu(II) biosorption from aqueous solutions using sugar beet shreds in a fixed-bed column, J. Hazard. Mater. 363 (2019) 366–375. https://doi.org/10.1016/j.jhazmat.2018.09.068.

[58] M. Ashrafi, H. Borzuie, G. Bagherian, M.A. Chamjangali, H. Nikoofard, Artificial neural network and multiple linear regression for modeling sorption of Pb2+ ions from aqueous solutions onto modified walnut shell, Sep. Sci. Technol. 55 (2020) 222–233. https://doi.org/10.1080/01496395.2019.1577437.

[59] W.A.H. Altowayti, H.A. Algaifi, S.A. Bakar, S. Shahir, The adsorptive removal of As (III) using biomass of arsenic resistant Bacillus thuringiensis strain WS3: Characteristics and modelling studies, Ecotoxicol. Environ. Saf. 172 (2019) 176–185. https://doi.org/10.1016/j.ecoenv.2019.01.067.

[60] R.R. Siva Kiran, G.M. Madhu, S. V Satyanarayana, P. Kalpana, G. Subba Rangaiah, Applications of Box–Behnken experimental design coupled with artificial neural networks for biosorption of low concentrations of cadmium using Spirulina (Arthrospira) spp., Resour. Technol. 3 (2017) 113–123. https://doi.org/10.1016/j.reffit.2016.12.009.

[61] H. Esfandian, M. Parvini, B. Khoshandam, A. Samadi-Maybodi, Artificial neural network (ANN) technique for modeling the mercury adsorption from aqueous solution using Sargassum Bevanom algae, Desalin. Water Treat. 57 (2016) 17206–17219. https://doi.org/10.1080/19443994.2015.1086696.

[62] D.I. Mendoza-Castillo, H.E. Reynel-Ávila, F.J. Sánchez-Ruiz, R. Trejo-Valencia, J.E. Jaime-Leal, A. Bonilla-Petriciolet, Insights and pitfalls of artificial neural network modeling of competitive multi-metallic adsorption data, J. Mol. Liq. 251 (2018) 15–27. https://doi.org/10.1016/j.molliq.2017.12.030.

[63] M. Shanmugaprakash, S. Venkatachalam, K. Rajendran, A. Pugazhendhi, Biosorptive removal of Zn(II) ions by Pongamia oil cake (Pongamia pinnata) in batch and fixed-bed column studies using response surface methodology and artificial neural network, J. Environ. Manage. 227 (2018) 216–228. https://doi.org/10.1016/j.jenvman.2018.08.088.

[64] M. Bouhedda, S. Lefnaoui, S. Rebouh, M.M. Yahoum, Predictive model based on Adaptive Neuro-Fuzzy Inference System for estimation of Cephalexin adsorption on the Octenyl Succinic Anhydride starch, Chemom. Intell. Lab. Syst. 193 (2019) 103843. https://doi.org/10.1016/j.chemolab.2019.103843.

[65] M. Gar Alalm, M. Nasr, Artificial intelligence, regression model, and cost estimation for removal of chlorothalonil pesticide by activated carbon prepared from casuarina charcoal, Sustain. Environ. Res. 28 (2018) 101–110. https://doi.org/10.1016/j.serj.2018.01.003.

[66] M. Vakili, A. Mojiri, T. Kindaichi, G. Cagnetta, J. Yuan, B. Wang, A.S. Giwa, Cross-linked chitosan/zeolite as a fixed-bed column for organic micropollutants removal from aqueous solution, optimization with RSM and artificial neural network, J. Environ. Manage. 250 (2019) 109434. https://doi.org/10.1016/j.jenvman.2019.109434.

[67] I.C. Afolabi, S.I. Popoola, O.S. Bello, Machine learning approach for prediction of paracetamol adsorption efficiency on chemically modified orange peel, Spectrochim. Acta Part A Mol. Biomol. Spectrosc. 243 (2020) 118769. https://doi.org/10.1016/j.saa.2020.118769.

[68] A.S. Mahmoud, M.K. Mostafa, M. Nasr, Regression model, artificial intelligence, and cost estimation for phosphate adsorption using encapsulated nanoscale zero-valent iron, Sep. Sci. Technol. 54 (2019) 13–26. https://doi.org/10.1080/01496395.2018.1504799.

[69] A.S. Mahmoud, A. Ismail, M.K. Mostafa, M.S. Mahmoud, W. Ali, A.M. Shawky, Isotherm and kinetic studies for heptachlor removal from aqueous solution using Fe/Cu nanoparticles, artificial intelligence, and regression analysis, Sep. Sci. Technol. 55 (2020) 684–696. https://doi.org/10.1080/01496395.2019.1574832.

[70] A.M. Ghaedi, M. Ghaedi, A.R. Pouranfard, A. Ansari, Z. Avazzadeh, A. Vafaei, I. Tyagi, S. Agarwal, V.K. Gupta, Adsorption of Triamterene on multi-walled and single-walled carbon nanotubes: Artificial neural network modeling and genetic algorithm optimization, J. Mol. Liq. (2016) 654–665. https://doi.org/10.1016/j.molliq.2016.01.068.

[71] K.P. Singh, S. Gupta, P. Ojha, P. Rai, Predicting adsorptive removal of chlorophenol from aqueous solution using artificial intelligence based modeling approaches, Environ. Sci. Pollut. Res. 20 (2013) 2271–2287. https://doi.org/10.1007/s11356-012-1102-y.

[72] K. Sharafi, M. Pirsaheb, V.K. Gupta, S. Agarwal, M. Moradi, Y. Vasseghian, E.-N. Dragoi, Phenol adsorption on scoria stone as adsorbent - Application of response surface method and artificial neural networks, J. Mol. Liq. 274 (2019) 699–714. https://doi.org/10.1016/j.molliq.2018.11.006.

[73] B.S. Chittoo, C. Sutherland, Column breakthrough studies for the removal and recovery of phosphate by lime-iron sludge: Modeling and optimization using artificial neural network

and adaptive neuro-fuzzy inference system, Chinese J. Chem. Eng. 28 (2020) 1847–1859. https://doi.org/10.1016/j.cjche.2020.02.022.

[74] M.A. Dalhat, N.D. Mu'azu, M.H. Essa, Generalized decay and artificial neural network models for fixed-Bed phenolic compounds adsorption onto activated date palm biochar, J. Environ. Chem. Eng. (2020) 104711. https://doi.org/10.1016/j.jece.2020.104711.

[75] R. Mohammadzadeh Kakhki, M. Mohammadpoor, R. Faridi, M. Bahadori, The development of an artificial neural network – genetic algorithm model (ANN-GA) for the adsorption and photocatalysis of methylene blue on a novel sulfur–nitrogen co-doped Fe2O3 nanostructure surface, RSC Adv. 10 (2020) 5951–5960. https://doi.org/10.1039/C9RA10349J.

[76] O.M.L. Alharbi, Sorption, kinetic, thermodynamics and artificial neural network modelling of phenol and 3-amino-phenol in water on composite iron nano-adsorbent, J. Mol. Liq. 260 (2018) 261–269. https://doi.org/10.1016/j.molliq.2018.03.104.

[77] R. Khandanlou, H.R. Fard Masoumi, M.B. Ahmad, K. Shameli, M. Basri, K. Kalantari, Enhancement of heavy metals sorption via nanocomposites of rice straw and Fe3O4 nanoparticles using artificial neural network (ANN), Ecol. Eng. 91 (2016) 249–256. https://doi.org/10.1016/j.ecoleng.2016.03.012.

[78] R.R. Karri, J.N. Sahu, Process optimization and adsorption modeling using activated carbon derived from palm oil kernel shell for Zn (II) disposal from the aqueous environment using differential evolution embedded neural network, J. Mol. Liq. 265 (2018) 592–602. https://doi.org/10.1016/j.molliq.2018.06.040.

[79] M.K. Uddin, R.A.K. Rao, K.V. V Chandra Mouli, The artificial neural network and Box-Behnken design for Cu2+ removal by the pottery sludge from water samples: Equilibrium, kinetic and thermodynamic studies, J. Mol. Liq. 266 (2018) 617–627. https://doi.org/10.1016/j.molliq.2018.06.098.

[80] S.K. Bhagat, T.M. Tung, Z.M. Yaseen, Development of artificial intelligence for modeling wastewater heavy metal removal: State of the art, application assessment and possible future research, J. Clean. Prod. 250 (2020) 119473. https://doi.org/10.1016/j.jclepro.2019.119473.

[81] S.A. Naghibi, E. Salehi, M. Khajavian, V. Vatanpour, M. Sillanpää, Multivariate data-based optimization of membrane adsorption process for wastewater treatment: Multi-layer

perceptron adaptive neural network versus adaptive neural fuzzy inference system, Chemosphere. 267 (2021) 129268. https://doi.org/10.1016/j.chemosphere.2020.129268.

[82] M.R. Sabour, A. Amiri, Comparative study of ANN and RSM for simultaneous optimization of multiple targets in Fenton treatment of landfill leachate, Waste Manag. 65 (2017) 54–62. https://doi.org/10.1016/j.wasman.2017.03.048.

[83] Y. Man, Y. Hu, J. Ren, Forecasting COD load in municipal sewage based on ARMA and VAR algorithms, Resour. Conserv. Recycl. 144 (2019) 56–64. https://doi.org/10.1016/j.resconrec.2019.01.030.

[84] P. Antwi, D. Zhang, L. Xiao, F.T. Kabutey, F.K. Quashie, W. Luo, J. Meng, J. Li, Modeling the performance of Single-stage Nitrogen removal using Anammox and Partial nitritation (SNAP) process with backpropagation neural network and response surface methodology, Sci. Total Environ. 690 (2019) 108–120. https://doi.org/10.1016/j.scitotenv.2019.06.530.

[85] F. Schmitt, K.-U. Do, Prediction of membrane fouling using artificial neural networks for wastewater treated by membrane bioreactor technologies: bottlenecks and possibilities, Environ. Sci. Pollut. Res. 24 (2017) 22885–22913. https://doi.org/10.1007/s11356-017-0046-7.

[86] S. Mandal, S.S. Mahapatra, S. Adhikari, R.K. Patel, Modeling of arsenic (III) removal by evolutionary genetic programming and least square support vector machine models, Environ. Process. 2 (2015) 145–172. https://doi.org/10.1007/s40710-014-0050-6.

[87] S. Mohan, Y. Singh, D.K. Verma, S.H. Hasan, Synthesis of CuO nanoparticles through green route using Citrus limon juice and its application as nanosorbent for Cr(VI) remediation: Process optimization with RSM and ANN-GA based model, Process Saf. Environ. Prot. 96 (2015) 156–166. https://doi.org/10.1016/j.psep.2015.05.005.

[88] M. Zafar, N. Van Vinh, S.K. Behera, H.-S. Park, Ethanol mediated As(III) adsorption onto Zn-loaded pinecone biochar: Experimental investigation, modeling, and optimization using hybrid artificial neural network-genetic algorithm approach, J. Environ. Sci. 54 (2017) 114–125. https://doi.org/10.1016/j.jes.2016.06.008.

[89] M. Fan, J. Hu, R. Cao, K. Xiong, X. Wei, Modeling and prediction of copper removal from aqueous solutions by nZVI/rGO magnetic nanocomposites using ANN-GA and ANN-PSO, Sci. Rep. 7 (2017) 18040. https://doi.org/10.1038/s41598-017-18223-y.

[90] F.S. Hoseinian, B. Rezai, E. Kowsari, The nickel ion removal prediction model from aqueous solutions using a hybrid neural genetic algorithm, J. Environ. Manage. 204 (2017) 311–317. https://doi.org/10.1016/j.jenvman.2017.09.011.

[91] S. Nag, A. Mondal, D.N. Roy, N. Bar, S.K. Das, Sustainable bioremediation of Cd (II) from aqueous solution using natural waste materials: kinetics, equilibrium, thermodynamics, toxicity studies and GA-ANN hybrid modelling, Environ. Technol. Innov. 11 (2018) 83–104. https://doi.org/10.1016/j.eti.2018.04.009.

[92] E.A. Dil, M. Ghaedi, A. Asfaram, The performance of nanorods material as adsorbent for removal of azo dyes and heavy metal ions: Application of ultrasound wave, optimization and modeling, Ultrason. Sonochem. 34 (2017) 792–802. https://doi.org/10.1016/j.ultsonch.2016.07.015.

[93] M. Ghaedi, A. Daneshfar, A. Ahmadi, M.S. Momeni, Artificial neural network-genetic algorithm based optimization for the adsorption of phenol red (PR) onto gold and titanium dioxide nanoparticles loaded on activated carbon, J. Ind. Eng. Chem. 21 (2015) 587–598. https://doi.org/10.1016/j.jiec.2014.03.024.

[94] M. Maghsoudi, M. Ghaedi, A. Zinali, A.M. Ghaedi, M.H. Habibi, Artificial neural network (ANN) method for modeling of sunset yellow dye adsorption using zinc oxide nanorods loaded on activated carbon: Kinetic and isotherm study, Spectrochim. Acta Part A Mol. Biomol. Spectrosc. 134 (2015) 1–9. https://doi.org/10.1016/j.saa.2014.06.106.

[95] A.A. Babaei, A. Khataee, E. Ahmadpour, M. Sheydaei, B. Kakavandi, Z. Alaee, Optimization of cationic dye adsorption on activated spent tea: equilibrium, kinetics, thermodynamic and artificial neural network modeling, Korean J. Chem. Eng. 33 (2016) 1352–1361. https://doi.org/10.1007/s11814-014-0334-6.

[96] A. Debnath, K. Deb, N.S. Das, K.K. Chattopadhyay, B. Saha, Simple Chemical Route Synthesis of Fe2O3 Nanoparticles and its Application for Adsorptive Removal of Congo Red from Aqueous Media: Artificial Neural Network Modeling, J. Dispers. Sci. Technol. 37 (2016) 775–785. https://doi.org/10.1080/01932691.2015.1062772.

[97] E.A. Dil, M. Ghaedi, A. Ghaedi, A. Asfaram, M. Jamshidi, M.K. Purkait, Application of artificial neural network and response surface methodology for the removal of crystal violet by zinc oxide nanorods loaded on activate carbon: kinetics and equilibrium study, J. Taiwan Inst. Chem. Eng. 59 (2016) 210–220. https://doi.org/10.1016/j.jtice.2015.07.023.

[98] A. Çelekli, H. Bozkurt, F. Geyik, Artificial neural network and genetic algorithms for modeling of removal of an azo dye on walnut husk, Desalin. Water Treat. 57 (2016) 15580–15591. https://doi.org/10.1080/19443994.2015.1070759.

[99] B. Heibati, S. Rodriguez-Couto, O. Ozgonenel, N.G. Turan, A. Aluigi, M.A. Zazouli, M.G. Ghozikali, M. Mohammadyan, A.B. Albadarin, A modeling study by artificial neural network on ethidium bromide adsorption optimization using natural pumice and iron-coated pumice, Desalin. Water Treat. 57 (2016) 13472–13483. https://doi.org/10.1080/19443994.2015.1060906.

[100] M.R.R. Kooh, M.K. Dahri, L.B.L. Lim, L.H. Lim, O.A. Malik, Batch adsorption studies of the removal of methyl violet 2B by soya bean waste: isotherm, kinetics and artificial neural network modelling, Environ. Earth Sci. 75 (2016) 783. https://doi.org/10.1007/s12665-016-5582-9.

[101] Z.U. Ahmad, L. Yao, Q. Lian, F. Islam, M.E. Zappi, D.D. Gang, The use of artificial neural network (ANN) for modeling adsorption of sunset yellow onto neodymium modified ordered mesoporous carbon, Chemosphere. 256 (2020) 127081. https://doi.org/10.1016/j.chemosphere.2020.127081.

[102] C.C. Okoye, O.D. Onukwuli, C.F. Okey-Onyesolu, Predictive capability evaluation of RSM and ANN models in adsorptive treatment of crystal violet dye simulated wastewater using activated carbon prepared from Raphia hookeri seeds, J. Chinese Adv. Mater. Soc. 6 (2018) 478–496. ttps://doi.org/10.1080/22243682.2018.1497534.

[103] N. Parsazadeh, F. Yousefi, M. Ghaedi, K. Dashtian, F. Borousan, Preparation and characterization of monoliths HKUST-1 MOF via straightforward conversion of Cu(OH)2-based monoliths and its application for wastewater treatment: artificial neural network and central composite design modeling, New J. Chem. 42 (2018) 10327–10336. https://doi.org/10.1039/C8NJ01067F.

[104] A.R. Bagheri, M. Ghaedi, S. Hajati, A.M. Ghaedi, A. Goudarzi, A. Asfaram, Random forest model for the ultrasonic-assisted removal of chrysoidine G by copper sulfide nanoparticles loaded on activated carbon; response surface methodology approach, RSC Adv. 5 (2015) 59335–59343. https://doi.org/10.1039/C5RA08399K.

[105] E. Oguz, Fixed-bed column studies on the removal of Fe3+ and neural network modelling, Arab. J. Chem. 10 (2017) 313–320. https://doi.org/10.1016/j.arabjc.2014.10.008.

[106] L.E. Hernández-Hernández, A. Bonilla-Petriciolet, D.I. Mendoza-Castillo, H.E. Reynel-Ávila, Antagonistic binary adsorption of heavy metals using stratified bone char columns, J. Mol. Liq. 241 (2017) 334–346. https://doi.org/10.1016/j.molliq.2017.05.148.

[107] S.S. Fiyadh, M.A. AlSaadi, M.K. AlOmar, S.S. Fayaed, A.R. Hama, S. Bee, A. El-Shafie, The modelling of lead removal from water by deep eutectic solvents functionalized CNTs: artificial neural network (ANN) approach, Water Sci. Technol. 76 (2017) 2413–2426. https://doi.org/10.2166/wst.2017.393%0A.

[108] E.A. Dil, M. Ghaedi, A. Asfaram, S. Hajati, F. Mehrabi, A. Goudarzi, Preparation of nanomaterials for the ultrasound-enhanced removal of Pb2+ ions and malachite green dye: chemometric optimization and modeling, Ultrason. Sonochem. 34 (2017) 677–691. https://doi.org/10.1016/j.ultsonch.2016.07.001.

[109] S.K. Ashan, N. Ziaeifar, R. Khalilnezhad, Artificial neural network modelling of Cr(VI) surface adsorption with NiO nanoparticles using the results obtained from optimization of response surface methodology, Neural Comput. Appl. 29 (2018) 969–979. https://doi.org/10.1007/s00521-017-3172-8.

[110] E. Allahkarami, A. Igder, A. Fazlavi, B. Rezai, Prediction of Co(II) and Ni(II) ions removal from wastewater using artificial neural network and multiple regression models, Physicochem. Probl. Miner. Process. 53 (2017) 1105–1118. https://doi.org/10.5277/ppmp170233.

[111] S. Varshney, P. Jain, J.K. Arora, S. Srivastava, Process development for the removal of toxic metals by functionalized wood pulp: kinetic, thermodynamic, and computational modeling approach, Clean Technol. Environ. Policy. 18 (2016) 2613–2623. https://doi.org/10.1007/s10098-016-1175-2.

[112] F. Rahimpour, T. Shojaeimehr, M. Sadeghi, Biosorption of Pb(II) using Gundelia tournefortii: Kinetics, equilibrium, and thermodynamics, Sep. Sci. Technol. 52 (2017) 596–607. https://doi.org/10.1080/01496395.2016.1260140.

[113] M.S. Podder, C.B. Majumder, The use of artificial neural network for modelling of phycoremediation of toxic elements As(III) and As(V) from wastewater using Botryococcus braunii, Spectrochim. Acta Part A Mol. Biomol. Spectrosc. 155 (2016) 130–145. https://doi.org/10.1016/j.saa.2015.11.011.

[114] R. Gomez-Gonzalez, F.J. Cerino-Córdova, A.M. Garcia-León, E. Soto-Regalado, N.E.

Davila-Guzman, J.J. Salazar-Rabago, Lead biosorption onto coffee grounds: Comparative analysis of several optimization techniques using equilibrium adsorption models and ANN, J. Taiwan Inst. Chem. Eng. 68 (2016) 201–210. https://doi.org/10.1016/j.jtice.2016.08.038.

[115] A. Debnath, M. Majumder, M. Pal, N.S. Das, K.K. Chattopadhyay, B. Saha, Enhanced Adsorption of Hexavalent Chromium onto Magnetic Calcium Ferrite Nanoparticles: Kinetic, Isotherm, and Neural Network Modeling, J. Dispers. Sci. Technol. 37 (2016) 1806–1818. https://doi.org/10.1080/01932691.2016.1141100.

[116] S. Yildiz, Artificial neural network (ANN) approach for modeling Zn(II) adsorption in batch process, Korean J. Chem. Eng. 34 (2017) 2423–2434. https://doi.org/10.1007/s11814-017-0157-3.

[117] B. Singha, N. Bar, S.K. Das, The use of artificial neural network (ANN) for modeling of Pb(II) adsorption in batch process, J. Mol. Liq. 211 (2015) 228–232. https://doi.org/10.1016/j.molliq.2015.07.002.

[118] D. Podstawczyk, A. Witek-Krowiak, A. Dawiec, A. Bhatnagar, Biosorption of copper(II) ions by flax meal: Empirical modeling and process optimization by response surface methodology (RSM) and artificial neural network (ANN) simulation, Ecol. Eng. 83 (2015) 364–379. https://doi.org/10.1016/j.ecoleng.2015.07.004.

[119] M. Nasr, A.E.D. Mahmoud, M. Fawzy, A. Radwan, Artificial intelligence modeling of cadmium(II) biosorption using rice straw, Appl. Water Sci. 7 (2017) 823–831. https://doi.org/10.1007/s13201-015-0295-x.

[120] S. Mandal, S.S. Mahapatra, R.K. Patel, Enhanced removal of Cr(VI) by cerium oxide polyaniline composite: Optimization and modeling approach using response surface methodology and artificial neural networks, J. Environ. Chem. Eng. 3 (2015) 870–885. https://doi.org/10.1016/j.jece.2015.03.028.

[121] J.A. Rodríguez-Romero, D.I. Mendoza-Castillo, H.E. Reynel-Ávila, D.A. de Haro-Del Rio, L.M. González-Rodríguez, A. Bonilla-Petriciolet, C.J. Duran-Valle, K.I. Camacho-Aguilar, Preparation of a new adsorbent for the removal of arsenic and its simulation with artificial neural network-based adsorption models, J. Environ. Chem. Eng. 8 (2020) 103928. https://doi.org/10.1016/j.jece.2020.103928.

[122] D.S.P. Franco, F.A. Duarte, N.P.G. Salau, G.L. Dotto, Adaptive neuro-fuzzy inference

system (ANIFS) and artificial neural network (ANN) applied for indium (III) adsorption on carbonaceous materials, Chem. Eng. Commun. 206 (2019) 1452–1462. https://doi.org/10.1080/00986445.2019.1566129.

[123] R. Beigzadeh, S.O. Rastegar, Assessment of Cr(VI) Biosorption from Aqueous Solution by Artificial Intelligence, Chem. Methodol. 4 (2020) 181–190. https://doi.org/10.33945/SAMI/CHEMM.2020.2.8.

[124] M. Dolatabadi, M. Mehrabpour, M. Esfandyari, H. Alidadi, M. Davoudi, Modeling of simultaneous adsorption of dye and metal ion by sawdust from aqueous solution using of ANN and ANFIS, Chemom. Intell. Lab. Syst. 181 (2018) 72–78. https://doi.org/10.1016/j.chemolab.2018.07.012.

[125] F.N. Oskui, H. Aghdasinia, M.G. Sorkhabi, Modeling and optimization of chromium adsorption onto clay using response surface methodology, artificial neural network, and equilibrium isotherm models, Environ. Prog. Sustain. Energy. 38 (2019) e13260. https://doi.org/10.1002/ep.13260.

[126] S. Ullah, M.A. Assiri, A.G. Al-Sehemi, M.A. Bustam, M. Sagir, F.A. Abdulkareem, M.R. Raza, M. Ayoub, A. Irfan, Characteristically Insights, Artificial Neural Network (ANN), Equilibrium, and Kinetic Studies of Pb(II) Ion Adsorption on Rice Husks Treated with Nitric Acid, Int. J. Environ. Res. 14 (2020) 43–60. https://doi.org/10.1007/s41742-019-00235-3.

[127] S. Ullah, M.A. Assiri, M.A. Bustam, A.G. Al-Sehemi, F.A.A. Kareem, A. Irfan, Equilibrium, kinetics and artificial intelligence characteristic analysis for Zn(II) ion adsorption on rice husks digested with nitric acid, Paddy Water Environ. 18 (2020) 455–468. https://doi.org/10.1007/s10333-020-00794-8.

[128] L.T. Popoola, Nano-magnetic walnut shell-rice husk for Cd(II) sorption: design and optimization using artificial intelligence and design expert, Heliyon. 5 (2019) e02381. https://doi.org/10.1016/j.heliyon.2019.e02381.

[129] Y.J. Wong, S.K. Arumugasamy, C.H. Chung, A. Selvarajoo, V. Sethu, Comparative study of artificial neural network (ANN), adaptive neuro-fuzzy inference system (ANFIS) and multiple linear regression (MLR) for modeling of Cu (II) adsorption from aqueous solution using biochar derived from rambutan (Nephelium lappaceum) pee, Environ. Monit. Assess. 192 (2020) 439. https://doi.org/10.1007/s10661-020-08268-4.

[130] P. Moradi, S. Hayati, T. Ghahrizadeh, Modeling and optimization of lead and cobalt biosorption from water with Rafsanjan pistachio shell, using experiment based models of ANN and GP, and the grey wolf optimizer, Chemom. Intell. Lab. Syst. 202 (2020) 104041. https://doi.org/10.1016/j.chemolab.2020.104041.

[131] S. Chattoraj, N.K. Mondal, B. Das, P. Roy, B. Sadhukhan, Carbaryl removal from aqueous solution by Lemna major biomass using response surface methodology and artificial neural network, J. Environ. Chem. Eng. 2 (2014) 1920–1928. https://doi.org/10.1016/j.jece.2014.08.011.

[132] P.S. Pauletto, S.F. Lütke, G.L. Dotto, N.P.G. Salau, Forecasting the multicomponent adsorption of nimesulide and paracetamol through artificial neural network, Chem. Eng. J. (2020) 127527. https://doi.org/10.1016/j.cej.2020.127527.

[133] S. Mondal, K. Aikat, G. Halder, Optimization of ranitidine hydrochloride removal from simulated pharmaceutical waste by activated charcoal from mung bean husk using response surface methodology and artificial neural network, Desalin. Water Treat. 57 (2016) 18366–18378. https://doi.org/10.1080/19443994.2015.1088899.

[134] R.M. Aghav, S. Kumar, S.N. Mukherjee, Artificial neural network modeling in competitive adsorption of phenol and resorcinol from water environment using some carbonaceous adsorbents, J. Hazard. Mater. 188 (2011) 67–77. https://doi.org/10.1016/j.jhazmat.2011.01.067.

[135] Z. Shahryari, A. Sharifi, A. Mohebbi, Artificial neural network (ANN) approach for modeling and formulation of phenol adsorption onto activated carbon, J. Eng. Thermophys. 22 (2013) 322–336. https://doi.org/10.1134/S181023281304005X.

[136] N.K. Mondal, R. Bhaumik, B. Das, P. Roy, J.K. Datta, S. Bhattacharyya, S. Bhattacharjee, Neural network model and isotherm study for removal of phenol from aqueous solution by orange peel ash, Appl. Water Sci. 5 (2015) 271–282. https://doi.org/10.1007/s13201-014-0188-4.

[137] A.S. Mahmoud, M.K. Mostafa, S.A. Abdel-Gawad, Artificial intelligence for the removal of benzene, toluene, ethyl benzene and xylene (BTEX) from aqueous solutions using iron nanoparticles, Water Supply. 18 (2017) 1650–1663. https://doi.org/10.2166/ws.2017.225.

[138] Y. Zhang, B. Pan, Modeling batch and column phosphate removal by hydrated ferric oxide-based nanocomposite using response surface methodology and artificial neural

network, Chem. Eng. J. 249 (2014) 111–120. https://doi.org/10.1016/j.cej.2014.03.073.

[139] A. Asfaram, M. Ghaedi, M.H.A. Azqhandi, A. Goudarzi, M. Dastkhoon, Statistical experimental design, least squares-support vector machine (LS-SVM) and artificial neural network (ANN) methods for modeling the facilitated adsorption of methylene blue dye, RSC Adv. 6 (2016) 40502–40516. https://doi.org/10.1039/C6RA01874B.

[140] N.M. Mahmoodi, Z. Hosseinabadi-Farahani, F. Bagherpour, M.R. Khoshrou, H. Chamani, F. Forouzeshfar, Synthesis of CuO–NiO nanocomposite and dye adsorption modeling using artificial neural network, Desalin. Water Treat. 57 (2016) 17220–17229. https://doi.org/10.1080/19443994.2015.1086895.

[141] S. Ebrahimpoor, V. Kiarostami, M. Khosravi, M. Davallo, A. Ghaedi, Bees metaheuristic algorithm with the aid of artificial neural networks for optimization of acid red 27 dye adsorption onto novel polypyrrole/SrFe12O19/graphene oxide nanocomposite, Polym. Bull. 76 (2019) 6529–6553. https://doi.org/10.1007/s00289-019-02700-7.

[142] R.M. Kakhki, M. Mohammadpoor, R. Faridi, M. Bahadori, The development of an artificial neural network–genetic algorithm model (ANN-GA) for the adsorption and photocatalysis of methylene blue on a novel sulfur–nitrogen co-doped Fe2O3 nanostructure surface, RSC Adv. 10 (2020) 5951–5960. https://doi.org/10.1039/C9RA10349J.

[143] J. Qi, Y. Hou, J. Hu, W. Ruan, Y. Xiang, X. Wei, Decontamination of methylene Blue from simulated wastewater by the mesoporous rGO/Fe/Co nanohybrids: Artificial intelligence modeling and optimization, Mater. Today Commun. 24 (2020) 100709. https://doi.org/10.1016/j.mtcomm.2019.100709.

[144] W. Ruan, J. Hu, J. Qi, Y. Hou, R. Cao, X. Wei, Removal of crystal violet by using reduced-graphene-oxide-supported bimetallic Fe/Ni nanoparticles (rGO/Fe/Ni): Application of artificial intelligence modeling for the optimization process, Materials (Basel). 11 (2018) 865. https://doi.org/10.3390/ma11050865.

[145] R.M. Hlihor, M. Diaconu, F. Leon, S. Curteanu, T. Tavares, M. Gavrilescu, Experimental analysis and mathematical prediction of Cd(II) removal by biosorption using support vector machines and genetic algorithms, N. Biotechnol. 32 (2015) 358–368. https://doi.org/10.1016/j.nbt.2014.08.003.

[146] M. Solgi, T. Najib, S. Ahmadnejad, B. Nasernejad, Synthesis and characterization of

novel activated carbon from Medlar seed for chromium removal: Experimental analysis and modeling with artificial neural network and support vector regression, Resour. Technol. 3 (2017) 236–248. https://doi.org/10.1016/j.reffit.2017.08.003.

[147] S. Nag, N. Bar, S.K. Das, Sustainable bioremadiation of Cd(II) in fixed bed column using green adsorbents: Application of Kinetic models and GA-ANN technique, Environ. Technol. Innov. 13 (2019) 130–145. https://doi.org/10.1016/j.eti.2018.11.007.

[148] M. Fan, J. Hu, R. Cao, W. Ruan, X. Wei, A review on experimental design for pollutants removal in water treatment with the aid of artificial intelligence, Chemosphere. 200 (2018) 330–343. https://doi.org/10.1016/j.chemosphere.2018.02.111.

Declaration of interests

☒ The authors declare that they have no known competing financial interests or personal relationships that could have appeared to influence the work reported in this paper.

☐The authors declare the following financial interests/personal relationships which may be considered as potential competing interests:

Highlights

- A comprehensive overview of AI applications in water treatment is presented.

- The potential of AI in predicting the uptake of various pollutants are portrayed in detail.
- The major challenges in AI applications are accentuated.
- A roadmap for future research is suggested.